MREP@60

A nonlinear pressure-driven laminar dynamo

Jonathan Mestel

Leszek Zabielski

Imperial College London

Warsaw University of Technology

Cargese, September 20, 2010

Outline

- **Motivation: Blood flow and MHD**
- **Helical Symmetry**
- **Single Pipe Dynamo**
- **Double-helix dynamo**
- **Multi-pipe dynamos**
- **Conclusions**

Birth of the idea. . .

Why look at flow down helical pipes?

The idea came from physiology:

Birth of the idea. . .

Birth of the idea. . .

The umbilical cord consists of a braid of two helical arteries and one vein.

Flows in helical, or three-dimensionally curved arteries have a number of physiological benefits.

Birth of the idea. . .

The umbilical cord consists of a braid of two helical arteries and one vein.
Flows in helical, or three-dimensionally curved arteries have a number of physiological benefits.

The baby girl was surely named

Dinah Michele Flo,
a clear pointer towards
Dynamic Heli-Flow.

So we replace her blood with liquid metal and reshape her arteries and consider flow through a helical pipe of rectangular cross-section.

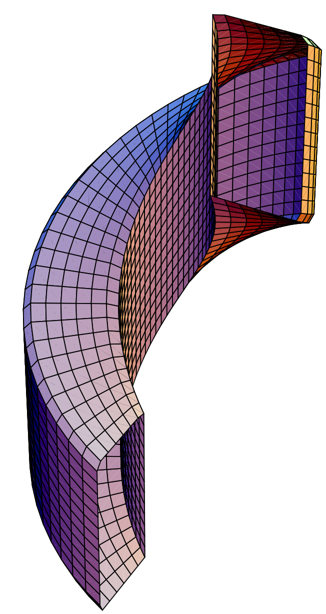

Two or more pipes

We may conveniently stack together two of these pipes like a barber's pole to form a complete annulus. These pipes are hydrodynamically separate, but electromagnetically linked.

The flow could go up one pipe and return through the other.

Similarly, we could fill an annulus with more than two helical ducts, down which we drive conducting fluid independently.

We might expect such helical flows to drive a dynamo in a manner reminiscent of the Riga and Karlsruhe experiments:

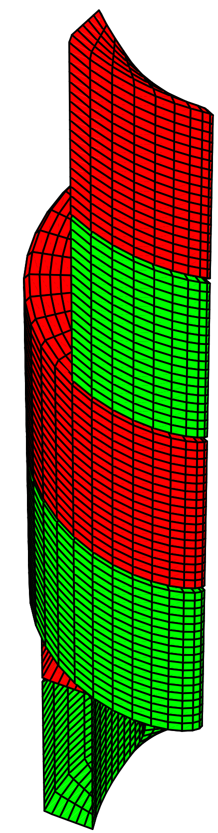

Karlsruhe experiment

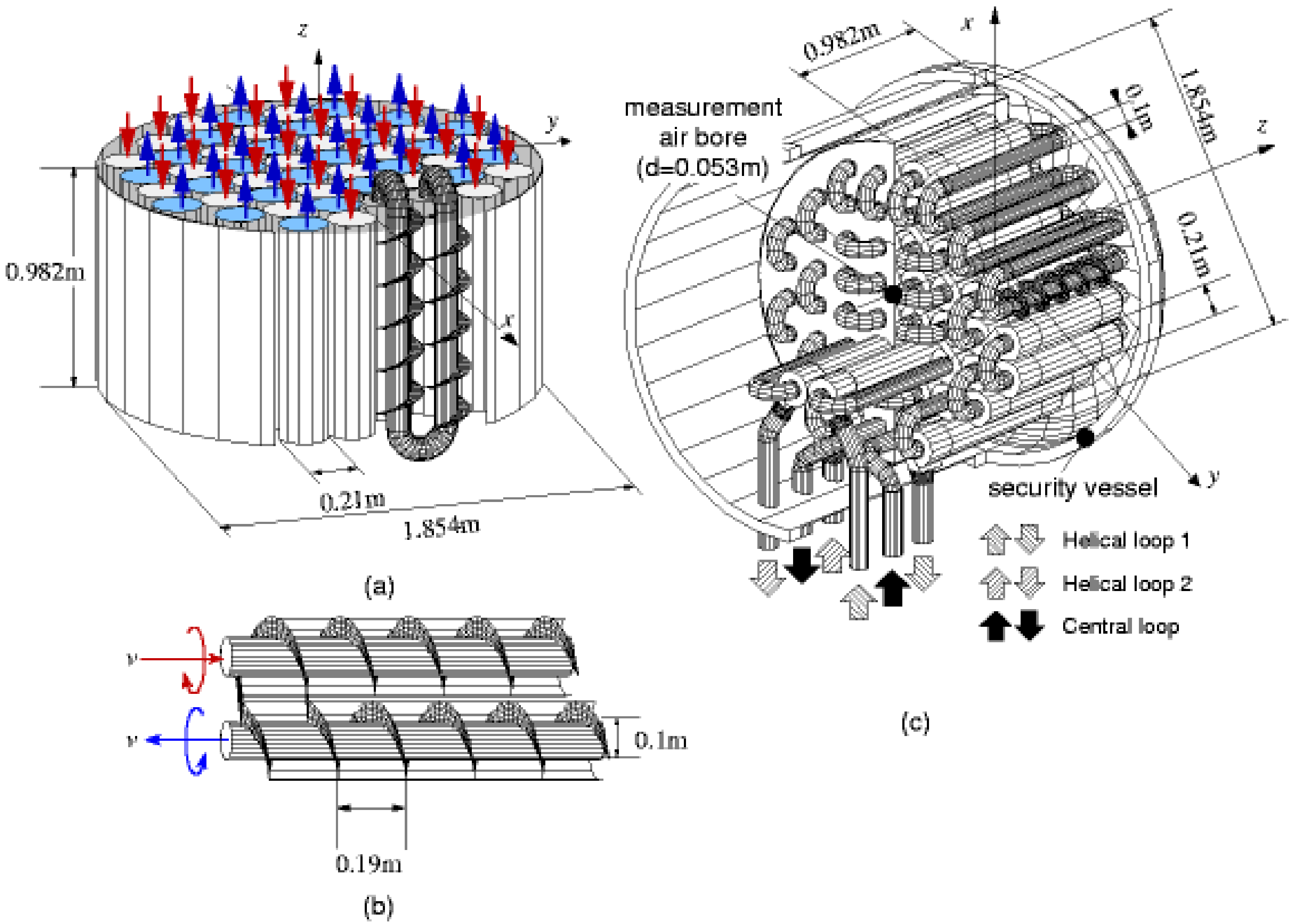

Riga experiment

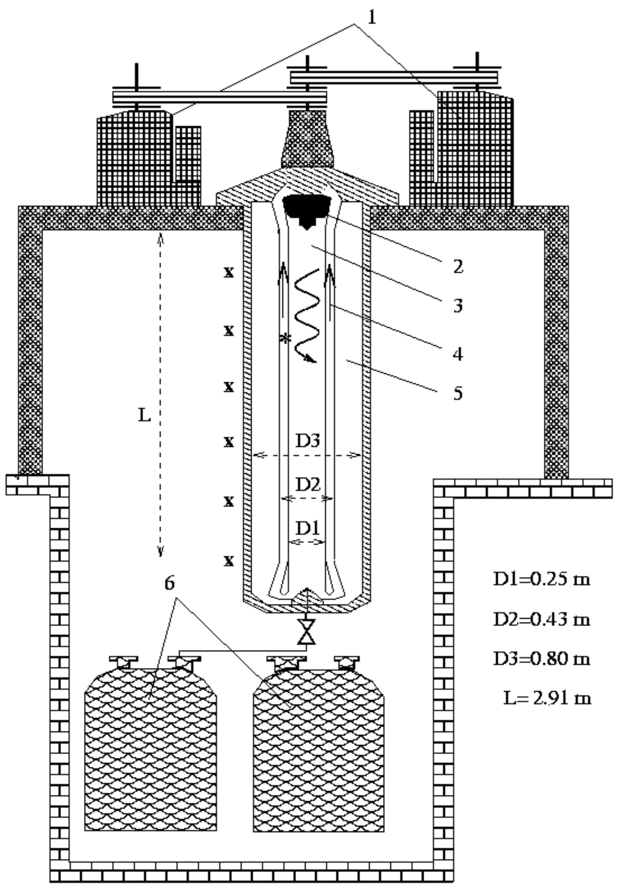

The Riga dynamo facility:
1 - Two motors (55 kW each),
2 - Propeller,
3 - Spiral flow,
4 - Back-flow,
5- Sodium at rest,
∗ - Flux-gate sensor, x - Six Hall

The kinematic dynamo problem

The induction equation:

$$\frac{\partial \mathbf{B}}{\partial t} = \nabla \times (\mathbf{u} \times \mathbf{B}) + \eta \nabla^2 \mathbf{B}$$

Kinematic dynamo question: Can a given flow $\mathbf{u}$ generate an unboundedly growing magnetic field $\mathbf{B}$ from some small initial disturbance?

Cowling's Antidynamo Theorem:
Neither fully axisymmetric nor 2-dimensional magnetic fields can be maintained by dynamo action.

But there is no bar to helically symmetric dynamos, with both $\mathbf{u}$ and $\mathbf{B}$ helically symmetric.

Helically symmetric dynamos are slow.
If

$$\mathbf{B} \propto e^{\lambda t} \qquad \text{then } \Re e[\lambda] \to 0 \text{ as } \eta \to 0.$$

Nonlinear dynamo problem

We seek to solve the coupled system:

$$\frac{\partial \mathbf{u}}{\partial t} + \mathbf{u}\cdot\nabla\mathbf{u} = -\nabla p + \nu\nabla^2\mathbf{u} + \mathbf{j}\times\mathbf{B}, \qquad \nabla\cdot\mathbf{u} = 0,$$

$$\frac{\partial \mathbf{B}}{\partial t} = \nabla\times(\mathbf{u}\times\mathbf{B}) + \eta\nabla^2\mathbf{B}, \qquad \nabla\cdot\mathbf{B} = 0.$$

We write $\nu = R_e^{-1}$ and $\eta = R_m^{-1}$.

In purely kinematic dynamos such as the Ponomarenko (1973), and Roberts (1972) dynamos the flow is prescribed rather than found dynamically and so the nonlinear problem can only be formulated by introducing a fictitious force.

Simple dynamo models which extend into the nonlinear regime are rare. Nonlinear dynamos usually require another process e.g.

- convection driven dynamos Matthews (1999), Kim *et al* (1999)
- moving boundaries e.g. Taylor-Couette flow: Bassom-Gilbert (1997), Dobler *et al* (2003).

Helical pipe dynamos

- Laminar, incompressible flow is driven down a helical pipe of rectangular cross-section by a pressure gradient with no slip on the wall.
- Helical symmetry is imposed on both the magnetic and the velocity fields.
- The dynamos are fully nonlinear exact solutions; no turbulent α-effect or artificial body force.
- Motivation: the helical geometry in Karlsruhe and Riga experiments;
- NOTE: We are using the word helical in an exact sense, which we now define.

Helical symmetry

Lortz (1968), Benton (1979) Childress *et al* (1989), Landman (1990), Dritschel (1991), Zabielski & Mestel (1998)

In terms of cylindrical polar coordinates $(r,\, \theta,\, z)$, the helical symmetry direction **H** is given by

$$\mathbf{H} = \frac{1}{h^2}(-\varepsilon r \mathbf{e}_\theta + \mathbf{e}_z) \qquad h = (1+\varepsilon^2 r^2)^{1/2}$$

The constant ε measures the pitch of a given helical line.

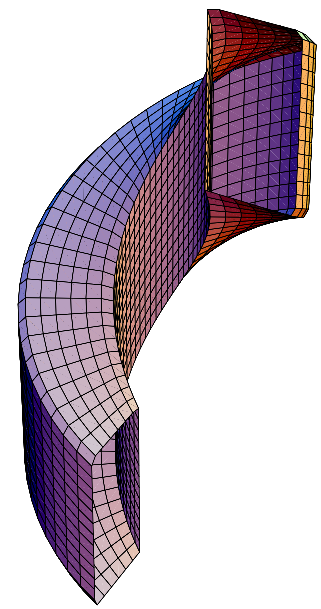

Helical pipe $\varepsilon = 1$, $b = 2$, $\phi_0 = 2\pi/3$

Helical symmetry

Lortz (1968), Benton (1979) Childress *et al* (1989),
Landman (1990), Dritschel (1991),
Zabielski & Mestel (1998)

In terms of cylindrical polar coordinates (r, θ, z), the helical symmetry direction **H** is given by

$$\mathbf{H} = \frac{1}{h^2}(-\varepsilon r \mathbf{e}_\theta + \mathbf{e}_z) \qquad h = (1 + \varepsilon^2 r^2)^{1/2}$$

The constant ε measures the pitch of a given helical line.

$\mathbf{H}$ is a non-unit Beltrami field

$$\nabla \times \mathbf{H} = -\frac{2\varepsilon}{h^2}\mathbf{H},$$

This Beltrami property is responsible for genuinely three-dimensional behaviour.

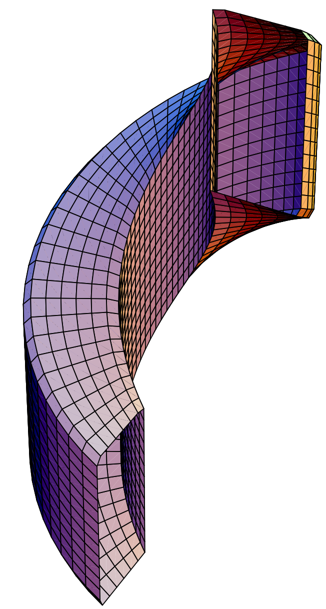

Helical pipe $\varepsilon = 1$, $b = 2$, $\phi_0 = 2\pi/3$

Helical symmetry

Lortz (1968), Benton (1979) Childress *et al* (1989), Landman (1990), Dritschel (1991), Zabielski & Mestel (1998)

In terms of cylindrical polar coordinates $(r,\ \theta,\ z)$, the helical symmetry direction $\mathbf{H}$ is given by

$$\mathbf{H} = \frac{1}{h^2}(-\varepsilon r \mathbf{e}_\theta + \mathbf{e}_z) \qquad h = (1+\varepsilon^2 r^2)^{1/2}$$

The constant ε measures the pitch of a given helical line.

$\mathbf{H}$ is a non-unit Beltrami field

$$\nabla \times \mathbf{H} = -\frac{2\varepsilon}{h^2}\mathbf{H},$$

A scalar function f is helically symmetric when

$$f = f(r,\phi) \qquad \phi = \theta + \varepsilon z$$

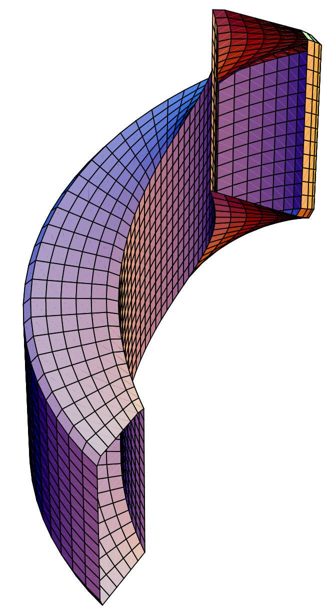

Helical pipe $\varepsilon = 1$, $b = 2$, $\phi_0 = 2\pi/3$

Helical symmetry

Lortz (1968), Benton (1979) Childress *et al* (1989), Landman (1990), Dritschel (1991), Zabielski & Mestel (1998)

In terms of cylindrical polar coordinates $(r,\,\theta,\,z)$, the helical symmetry direction **H** is given by

$$\mathbf{H} = \frac{1}{h^2}(-\varepsilon r \mathbf{e}_\theta + \mathbf{e}_z) \qquad h = (1+\varepsilon^2 r^2)^{1/2}$$

The constant ε measures the pitch of a given helical line.

$\mathbf{H}$ is a non-unit Beltrami field

$$\nabla \times \mathbf{H} = -\frac{2\varepsilon}{h^2}\mathbf{H},$$

A scalar function f is helically symmetric when

$$f = f(r,\phi) \qquad \phi = \theta + \varepsilon z$$

In the limits

$$\varepsilon \to 0 \Rightarrow \mathbf{H} \to \mathbf{e}_z,$$
$$\varepsilon \to \infty \Rightarrow h\mathbf{H} \to -\mathbf{e}_\theta$$

so that helical symmetry simplifies to two-dimensionality ($\varepsilon = 0$) and axisymmetry ($\varepsilon \to \infty$).

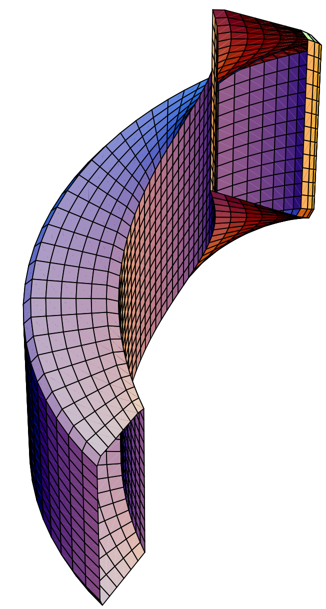

Helical pipe $\varepsilon = 1$, $b = 2$, $\phi_0 = 2\pi/3$

Representation of the velocity field

A helically symmetric solenoidal velocity field depends on two scalar functions $\Psi(r,\phi)$ and $v(r,\phi)$:

$$\mathbf{u} = \mathbf{H} \times \nabla\Psi + v\mathbf{H}$$

The vorticity vector field $\boldsymbol{\omega} = \nabla \times \mathbf{u}$

$$\boldsymbol{\omega} = \mathbf{H} \times \nabla(-v) + \xi\mathbf{H} \quad \text{where } \mathcal{L}\Psi = \frac{2\varepsilon}{h^2}v + \xi.$$

Navier-Stokes equations:

$$\frac{\partial v}{\partial t} + \frac{1}{r}J(\Psi,v) = G(t) + \nu(\mathcal{L}v + \frac{2\varepsilon}{h^2}\xi)$$

$$\frac{\partial \xi}{\partial t} + \left(-\frac{2\varepsilon}{h^2}\frac{1}{r}J(\Psi,v) + \frac{1}{r}J(\Psi,\xi) + \frac{2\varepsilon^2}{h^2}(\xi\frac{\partial\Psi}{\partial\phi} + v\frac{\partial v}{\partial\phi})\right) = \nu(\mathcal{L}\xi - \frac{2\varepsilon}{h^2}(\mathcal{L}v + \frac{2\varepsilon}{h^2}\xi))$$

$G(t)$ is the imposed down-pipe pressure gradient. In this talk, G is constant.

Representation of the velocity field

A helically symmetric solenoidal velocity field depends on two scalar functions $\Psi(r,\phi)$ and $v(r,\phi)$:

$$\mathbf{u} = \mathbf{H} \times \nabla\Psi + v\mathbf{H}$$

The vorticity vector field $\boldsymbol{\omega} = \nabla \times \mathbf{u}$

$$\boldsymbol{\omega} = \mathbf{H} \times \nabla(-v) + \xi\mathbf{H} \quad \text{where } \mathcal{L}\Psi = \frac{2\varepsilon}{h^2}v + \xi.$$

Navier-Stokes equations:

$$\frac{\partial v}{\partial t} + \frac{1}{r}J(\Psi,v) = G(t) + \nu(\mathcal{L}v + \frac{2\varepsilon}{h^2}\xi) - \left(\frac{1}{r}J(B,\chi)\right)$$

$$\frac{\partial \xi}{\partial t} + \left(-\frac{2\varepsilon}{h^2}\frac{1}{r}J(\Psi,v) + \frac{1}{r}J(\Psi,\xi) + \frac{2\varepsilon^2}{h^2}(\xi\frac{\partial\Psi}{\partial\phi} + v\frac{\partial v}{\partial\phi})\right) = \nu(\mathcal{L}\xi - \frac{2\varepsilon}{h^2}(\mathcal{L}v + \frac{2\varepsilon}{h^2}\xi))$$
$$+ \left(\frac{2\varepsilon}{h^2}\frac{1}{r}J(B,\chi) - \frac{1}{r}J(\gamma,\chi) - \frac{2\varepsilon^2}{h^2}\gamma\frac{\partial\chi}{\partial\phi} + \frac{2\varepsilon^2}{h^2}B\frac{\partial B}{\partial\phi}\right)$$

$G(t)$ is the imposed down-pipe pressure gradient. In this talk, G is constant.

Representation of the magnetic field

The helically symmetric solenoidal ($\nabla \cdot \mathbf{B} = 0$) magnetic field $\mathbf{B}$ can be represented by two helically symmetric scalar functions $\chi(r,\,\phi)$ and $B(r,\phi)$:

$$\mathbf{B} = \mathbf{H} \times \nabla\chi + B\mathbf{H}$$

analogously to the poloidal and toroidal components in axisymmetry. The current $\mathbf{j}$

$$\mathbf{j} = \nabla \times \mathbf{B} = \mathbf{H} \times \nabla(-B) + \gamma\mathbf{H} \quad \text{where } \mathcal{L}\chi = \frac{2\varepsilon}{h^2}B + \gamma.$$

Representation of the magnetic field

The helically symmetric solenoidal ($\nabla \cdot \mathbf{B} = 0$) magnetic field $\mathbf{B}$ can be represented by two helically symmetric scalar functions $\chi(r, \phi)$ and $B(r, \phi)$:

$$\mathbf{B} = \mathbf{H} \times \nabla\chi + B\mathbf{H}$$

analogously to the poloidal and toroidal components in axisymmetry. The current $\mathbf{j}$

$$\mathbf{j} = \nabla \times \mathbf{B} = \mathbf{H} \times \nabla(-B) + \gamma\mathbf{H} \quad \text{where } \mathcal{L}\chi = \frac{2\varepsilon}{h^2}B + \gamma.$$

The magnetic induction equation then takes the form:

$$\frac{\partial\chi}{\partial t} + \frac{1}{r}J(\Psi, \chi) = \eta\left(\mathcal{L}\chi - \frac{2\varepsilon}{h^2}B\right)$$

$$\frac{\partial B}{\partial t} + \left(\frac{2\varepsilon}{h^2}\frac{1}{r}J(\Psi, \chi) + \frac{h^2}{r}J(\frac{v}{h^2}, \chi) + \frac{h^2}{r}J\left(\Psi, \frac{B}{h^2}\right)\right) = \eta\left(\mathcal{L}B + \frac{2\varepsilon}{h^2}(\mathcal{L}\chi - \frac{2\varepsilon}{h^2}B)\right)$$

where the Jacobian $J(f, g) = \frac{\partial(f,g)}{\partial(r,\phi)}$ and the operator $\mathcal{L} = h^2\nabla \cdot \frac{1}{h^2}\nabla$.

Representation of the magnetic field

The helically symmetric solenoidal ($\nabla \cdot \mathbf{B} = 0$) magnetic field $\mathbf{B}$ can be represented by two helically symmetric scalar functions $\chi(r,\, \phi)$ and $B(r, \phi)$:

$$\mathbf{B} = \mathbf{H} \times \nabla\chi + B\mathbf{H}$$

analogously to the poloidal and toroidal components in axisymmetry. The current $\mathbf{j}$

$$\mathbf{j} = \nabla \times \mathbf{B} = \mathbf{H} \times \nabla(-B) + \gamma\mathbf{H} \quad \text{where } \mathcal{L}\chi = \frac{2\varepsilon}{h^2}B + \gamma.$$

The magnetic induction equation then takes the form:

$$\frac{\partial \chi}{\partial t} + \frac{1}{r}J(\Psi, \chi) = \eta\left(\mathcal{L}\chi - \frac{2\varepsilon}{h^2}B\right)$$

$$\frac{\partial B}{\partial t} + \left(\frac{2\varepsilon}{h^2}\frac{1}{r}J(\Psi, \chi) + \frac{h^2}{r}J(\frac{v}{h^2}, \chi) + \frac{h^2}{r}J\left(\Psi, \frac{B}{h^2}\right)\right) = \eta\left(\mathcal{L}B + \frac{2\varepsilon}{h^2}(\mathcal{L}\chi - \frac{2\varepsilon}{h^2}B)\right)$$

The blue term corresponds to differential rotation. The red term is especially important as it can generate poloidal field from toroidal field, a feature lacking in axisymmetry. As this term is multiplied by η, the dynamo is slow.

Steady helical pipe flow in a square pipe

The inside of the helical pipe is on the left.

cross-pipe streamlines | Downpipe flow $\mathbf{R_e = 13}$ | down-pipe vorticity

Ψ | v | ξ

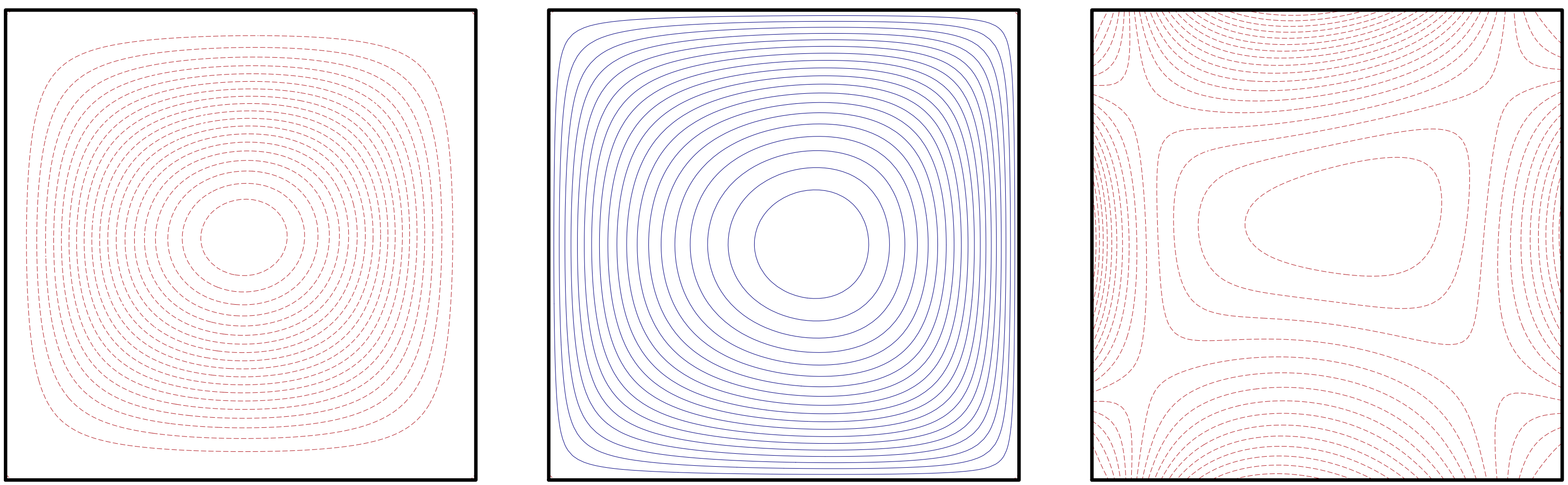

Steady helical pipe flow in a square pipe

The inside of the helical pipe is on the left.

cross-pipe streamlines	Downpipe flow $\mathbf{R_e = 37}$	down-pipe vorticity
Ψ	v	ξ

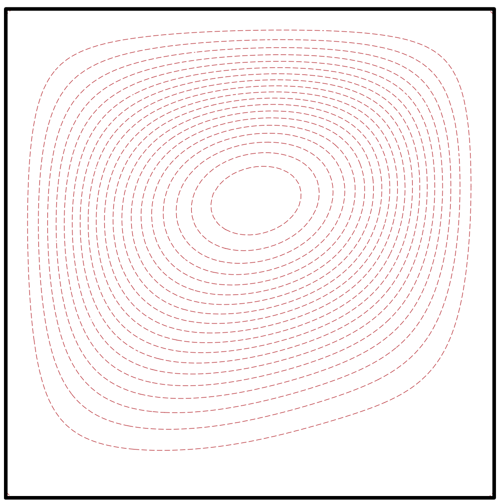

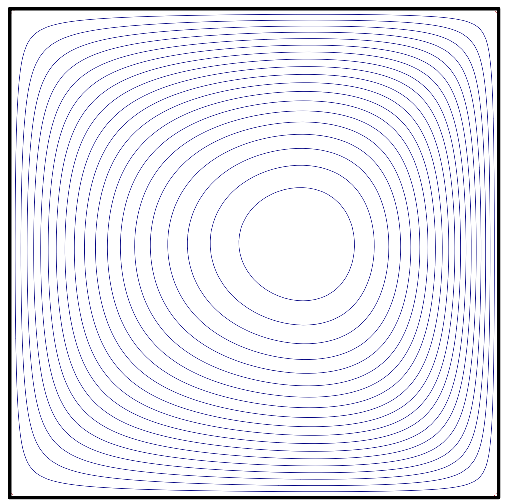

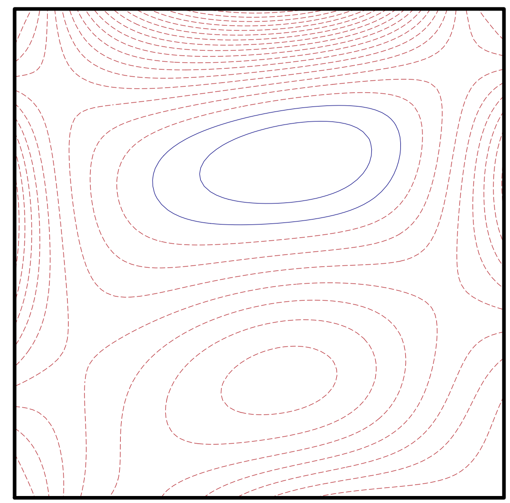

Steady helical pipe flow in a square pipe

The inside of the helical pipe is on the left.

cross-pipe streamlines	Downpipe flow $\mathbf{R_e = 43}$	down-pipe vorticity
Ψ	v	ξ

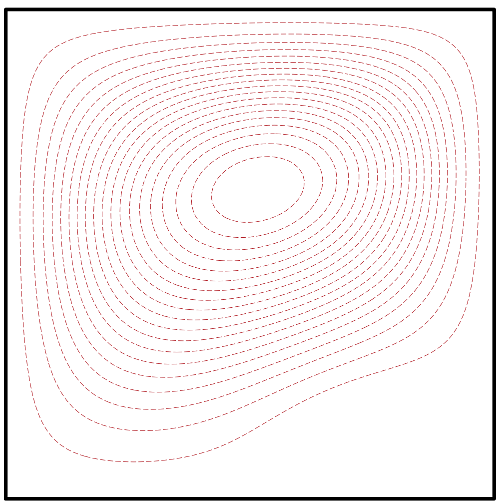

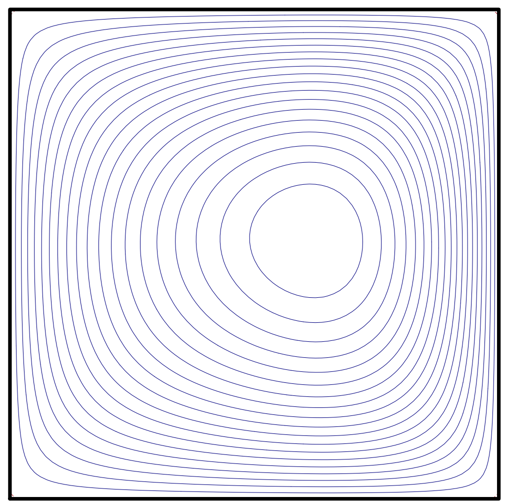

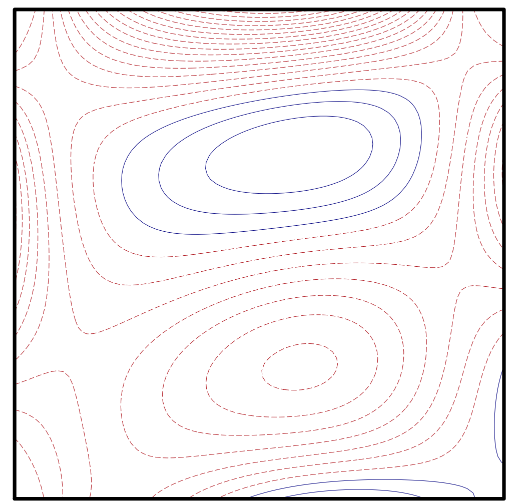

Steady helical pipe flow in a square pipe

The inside of the helical pipe is on the left.

cross-pipe streamlines	Downpipe flow $\mathbf{R_e = 49}$	down-pipe vorticity
Ψ	v	ξ

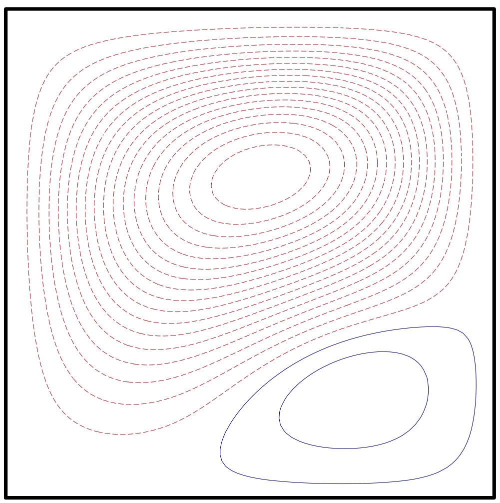

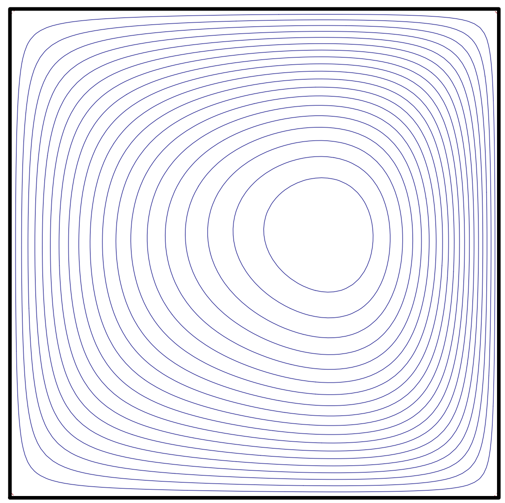

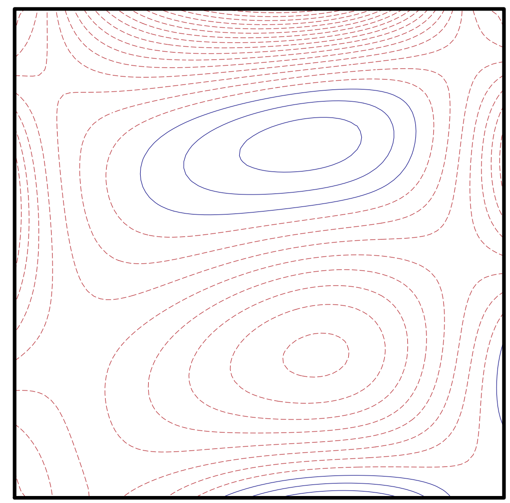

Steady helical pipe flow in a square pipe

The inside of the helical pipe is on the left.

cross-pipe streamlines	Downpipe flow $\mathbf{R_e = 69}$	down-pipe vorticity
Ψ	v	ξ

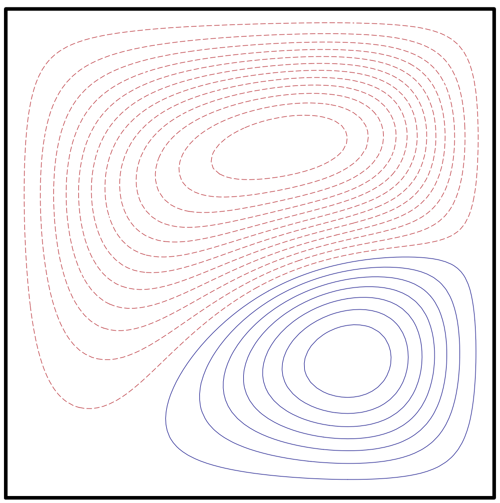

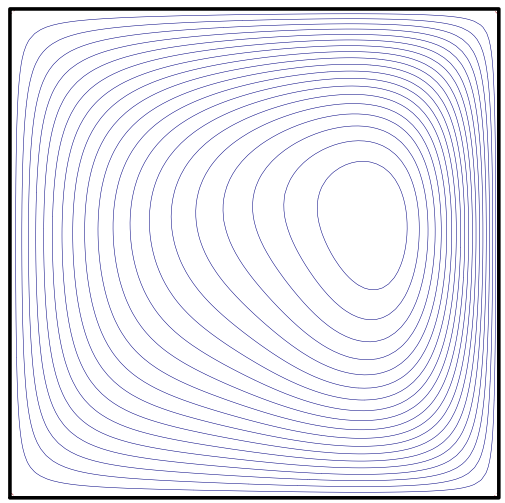

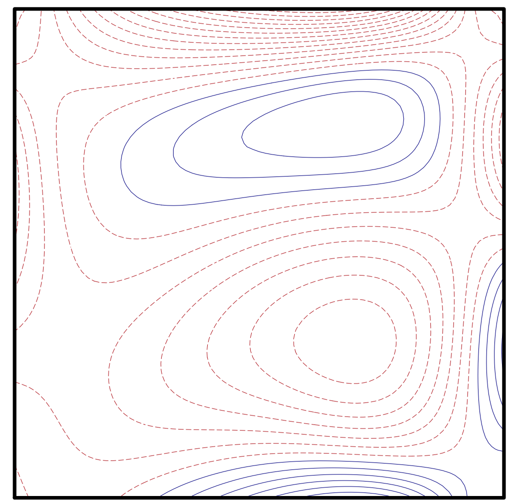

Steady helical pipe flow in a square pipe

The inside of the helical pipe is on the left.

cross-pipe streamlines	Downpipe flow $\mathbf{R_e = 106}$	down-pipe vorticity
Ψ	v	ξ
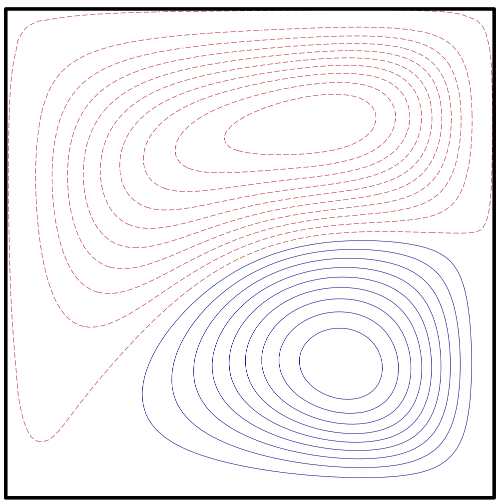	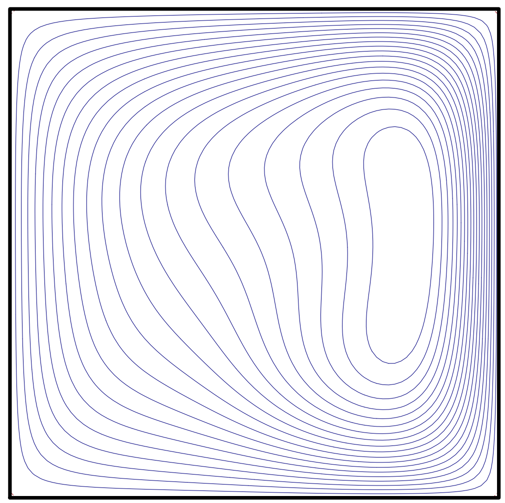	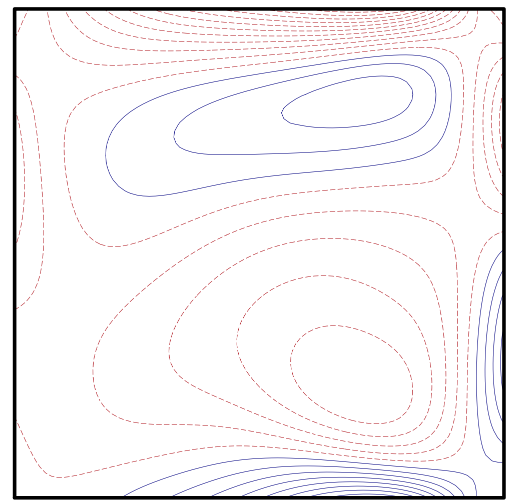

Steady helical pipe flow in a square pipe

The inside of the helical pipe is on the left.

cross-pipe streamlines

Downpipe flow
$\mathbf{R_e = 148}$

down-pipe vorticity

Ψ

v

ξ

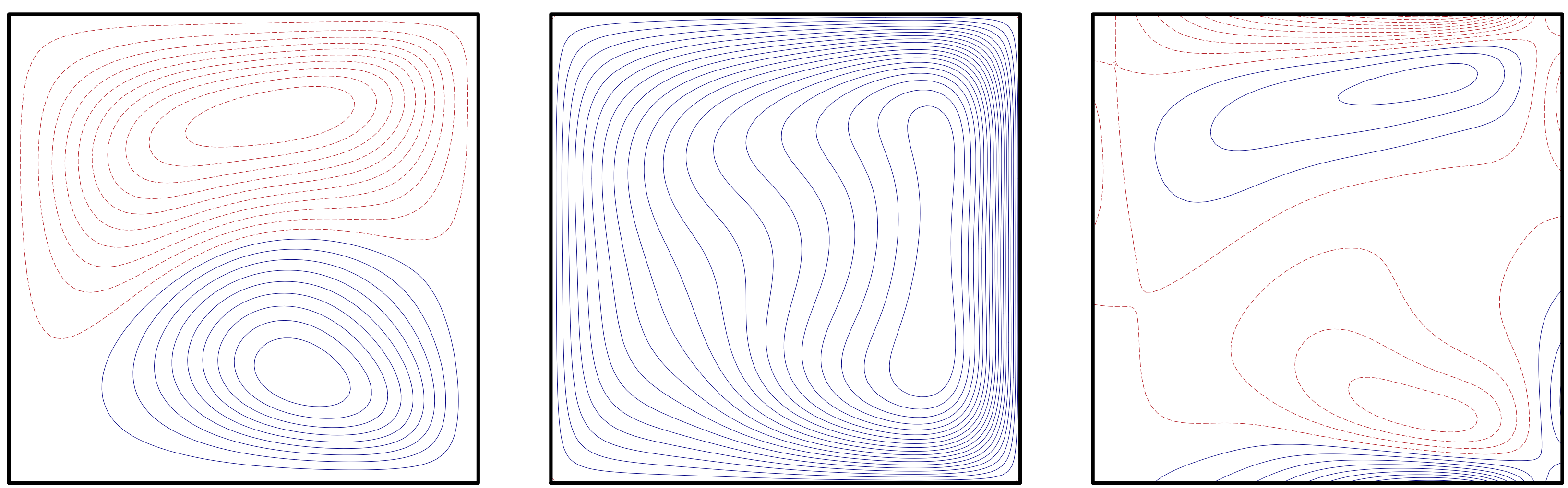

Steady helical pipe flow in a square pipe

The inside of the helical pipe is on the left.

cross-pipe streamlines	Downpipe flow $\mathbf{R_e = 195}$	down-pipe vorticity
Ψ	v	ξ

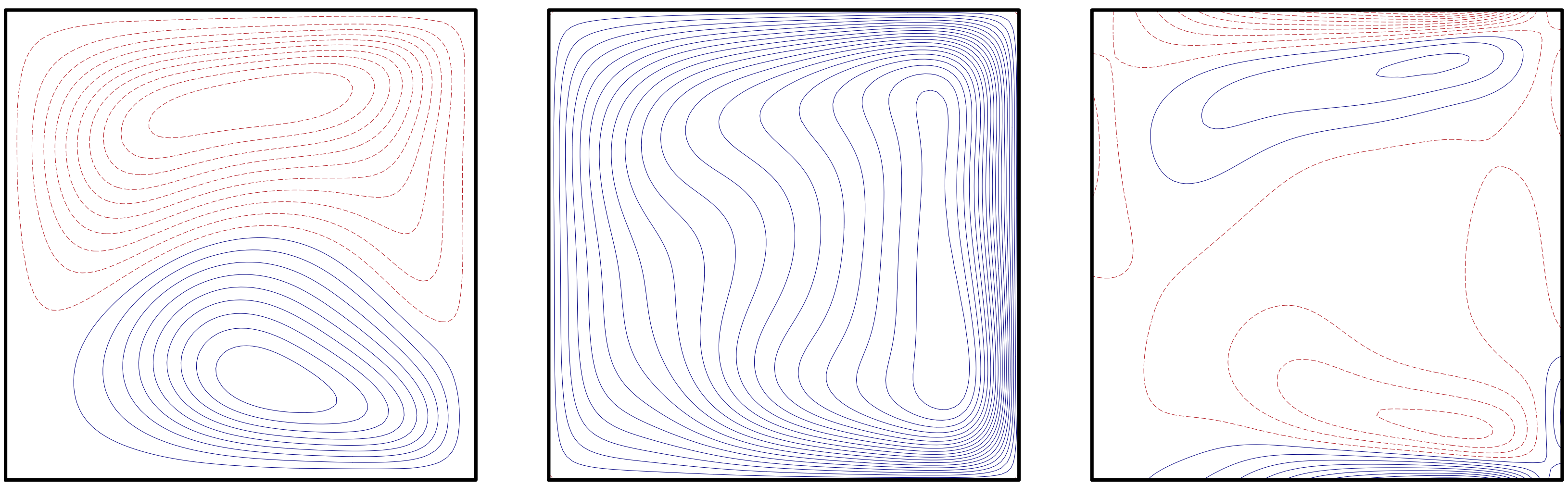

Asymptotics as $R_e \to \infty$ for axisymmetric ($\varepsilon \to \infty$) Dean flow (small curvature, pipe radius $b \to \infty$) Smith, F.T. (1976), Dennis & Riley (1991)

$\Psi \sim R_e^{\frac{1}{3}}$ $\quad v \sim R_e^{\frac{2}{3}}$ $\quad$ boundary layer $\sim R_e^{-\frac{1}{3}}$

Steady flow features

Solve the helical Navier-Stokes equations using finite differences.

At low Reynolds number cross-pipe flow is a single gyre (no dynamo)

Steady flow features

Solve the helical Navier-Stokes equations using finite differences.

At low Reynolds number cross-pipe flow is a single gyre (no dynamo) As R_e increases,

Steady flow features

Solve the helical Navier-Stokes equations using finite differences.

At low Reynolds number cross-pipe flow is a single gyre (no dynamo) As R_e increases,

- the cross-pipe structure changes from a single gyre to the double vortex associated with Dean flow.
- At higher R_e flow is nearly top down symmetric, and shows a core/boundary layer structure, again similar to Dean flow. Layers separate asymmetrically as the inner bend is approached.
- Flow becomes time-dependent. Instability may be of Görtler type (curvature of outer wall) or due to inflection of cross-pipe flow (see later).

Magnetic boundary conditions

Dynamos have been found for

- insulating boundary conditions (external potential field)
- Same conductivity inside and out
- Perfectly conducting walls

Only perfectly conducting boundaries are considered here. This requires:

$$\chi = 0 \quad \text{and} \quad \mathbf{n} \cdot \nabla B = 0 \quad \text{on } S$$

Perfectly conducting walls imply conservation of total flux down the pipe. There is a neutral mode in this case.

Neutral mode for perfectly conducting walls

Does the steady helical pipe flow drive a dynamo?

For a single pipe, only for carefully chosen geometry and R_e.

E.g. For a helical pipe with square cross-section no growing magnetic field has been found: no dynamo.

Neutral mode for perfectly conducting walls

Does the steady helical pipe flow drive a dynamo?

For a single pipe, only for carefully chosen geometry and R_e.

E.g. For a helical pipe with square cross-section no growing magnetic field has been found: no dynamo.

The cross-pipe flow has a strong effect: Ψ dominates the structure of the magnetic field.

Neutral mode for perfectly conducting walls

Does the steady helical pipe flow drive a dynamo?

For a single pipe, only for carefully chosen geometry and R_e.

E.g. For a helical pipe with square cross-section no growing magnetic field has been found: no dynamo.

The cross-pipe flow has a strong effect: Ψ dominates the structure of the magnetic field.

$$\mathbf{R_m = 7^3 \ R_e = 106}$$

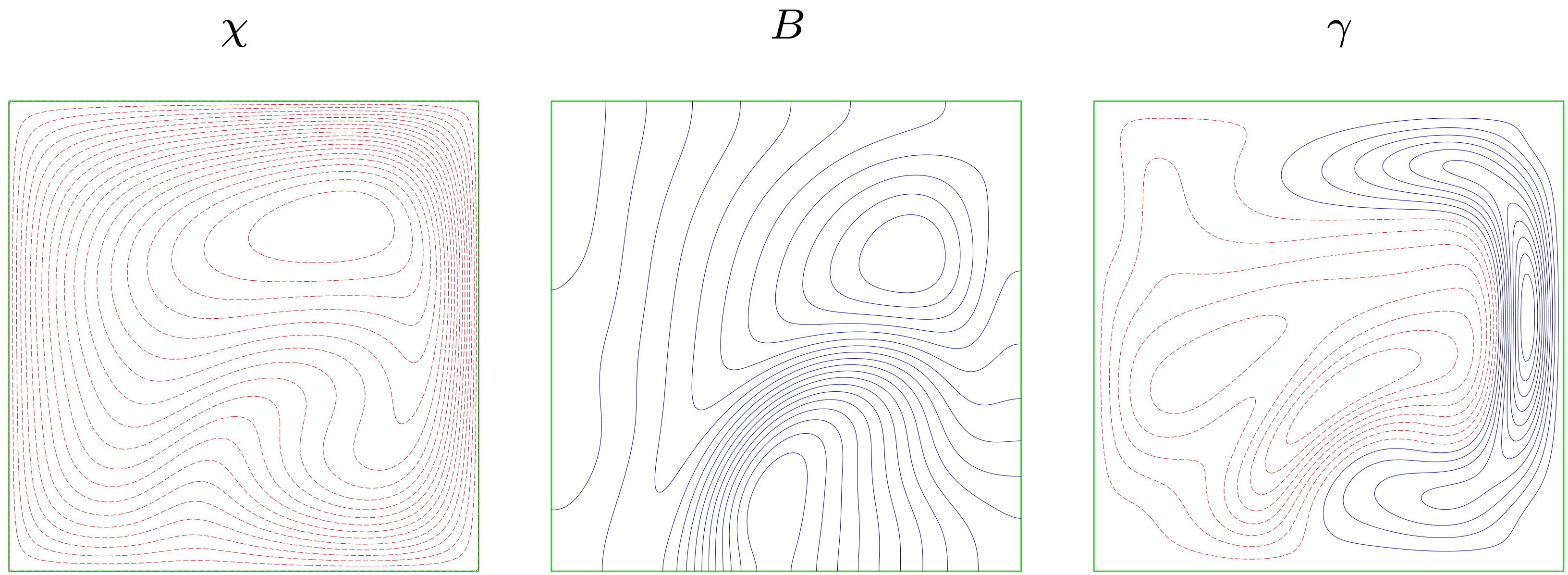

Neutral mode for perfectly conducting walls

Does the steady helical pipe flow drive a dynamo?

For a single pipe, only for carefully chosen geometry and R_e.

E.g. For a helical pipe with square cross-section no growing magnetic field has been found: no dynamo.

The cross-pipe flow has a strong effect: Ψ dominates the structure of the magnetic field.

$$\mathbf{R_m = 10^3 \ R_e = 106}$$

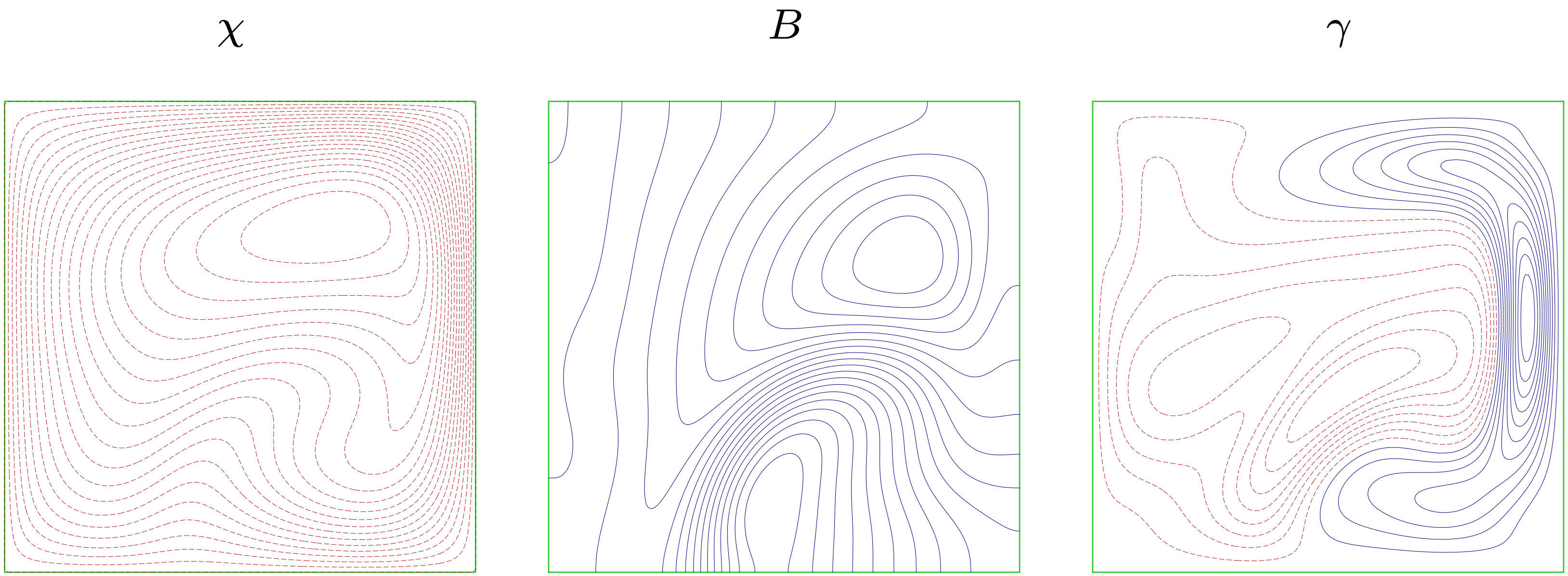

Neutral mode for perfectly conducting walls

Does the steady helical pipe flow drive a dynamo?

For a single pipe, only for carefully chosen geometry and R_e.

E.g. For a helical pipe with square cross-section no growing magnetic field has been found: no dynamo.

The cross-pipe flow has a strong effect: Ψ dominates the structure of the magnetic field.

$$\mathbf{R_m = 20^3 \ R_e = 106}$$

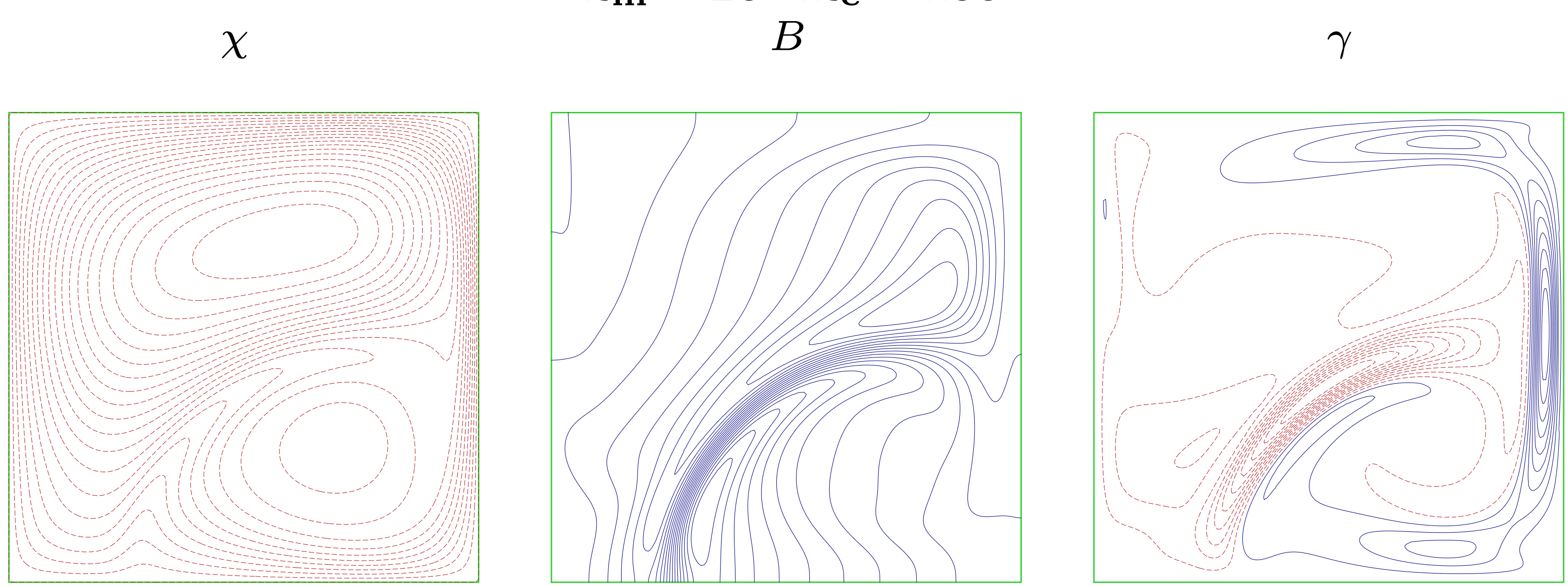

Neutral mode for perfectly conducting walls

Does the steady helical pipe flow drive a dynamo?

For a single pipe, only for carefully chosen geometry and R_e.

E.g. For a helical pipe with square cross-section no growing magnetic field has been found: no dynamo.

The cross-pipe flow has a strong effect: Ψ dominates the structure of the magnetic field.

$$\mathbf{R_m = 30^3 \; R_e = 106}$$

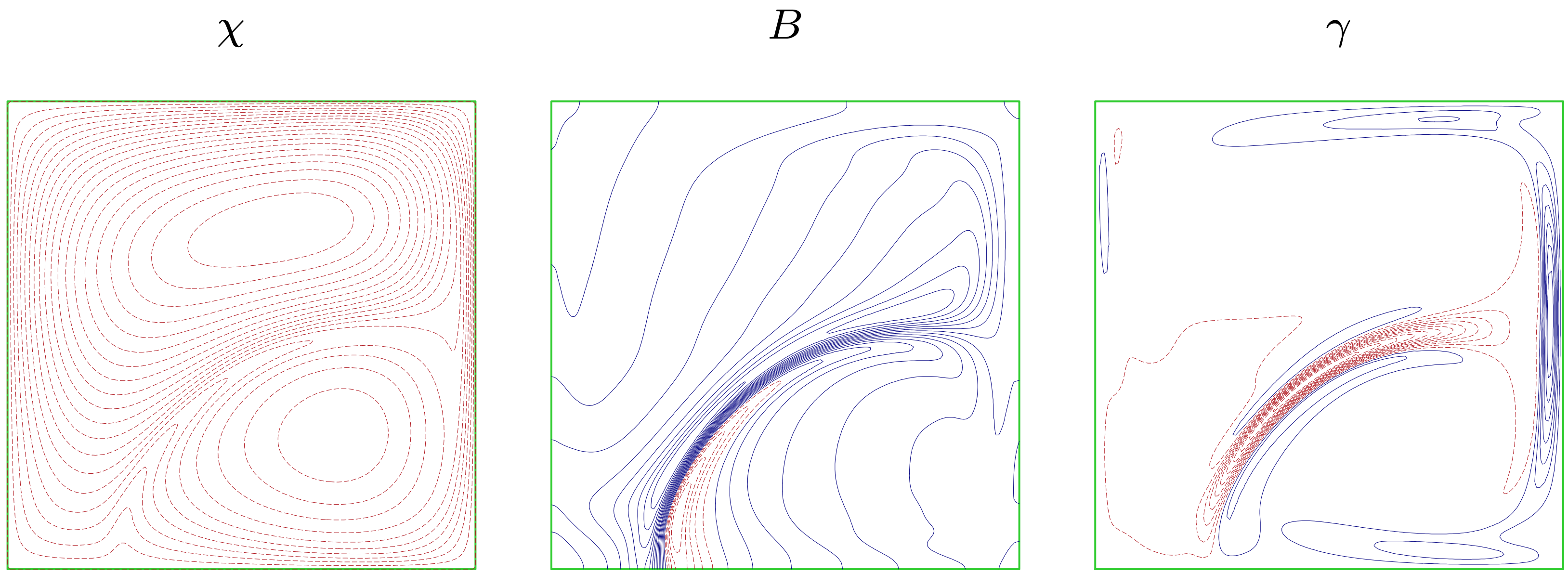

Neutral mode for perfectly conducting walls

Does the steady helical pipe flow drive a dynamo?

For a single pipe, only for carefully chosen geometry and R_e.

E.g. For a helical pipe with square cross-section no growing magnetic field has been found: no dynamo.

The cross-pipe flow has a strong effect: Ψ dominates the structure of the magnetic field.

Compare the flow pattern $\mathbf{R_e = 106}$

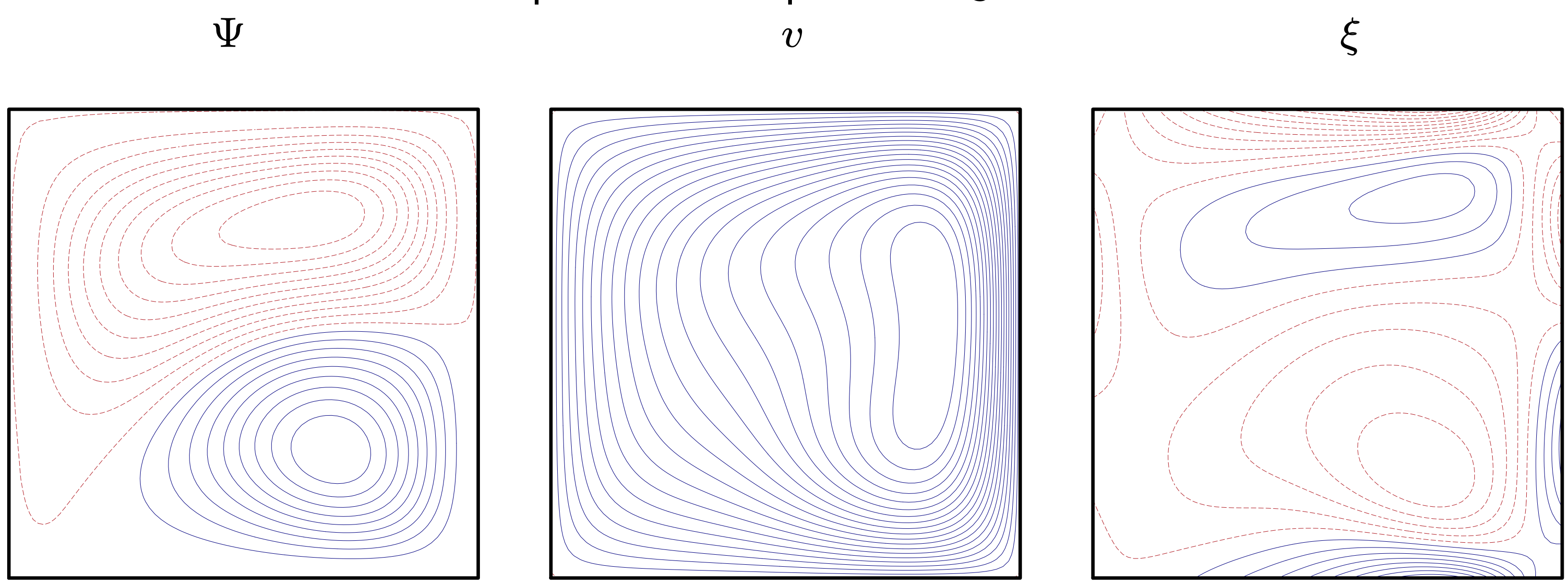

Neutral mode for perfectly conducting walls

Does the steady helical pipe flow drive a dynamo?

For a single pipe, only for carefully chosen geometry and R_e.

E.g. For a helical pipe with square cross-section no growing magnetic field has been found: no dynamo.

The cross-pipe flow has a strong effect: Ψ dominates the structure of the magnetic field.

Shear in downpipe flow v is good for the dynamo, but cross-pipe flow ψ opposes it.
Artificially switching off ψ leads to a dynamo, but for a Navier-Stokes solution, in a single pipe must choose pipe height and R_e to have a region of weak ψ.

Flow and hydrodynamic instability

Flow structure in the tall pipe $(\phi_0 = \pi)$

$$\mathbf{R_e = 13}$$

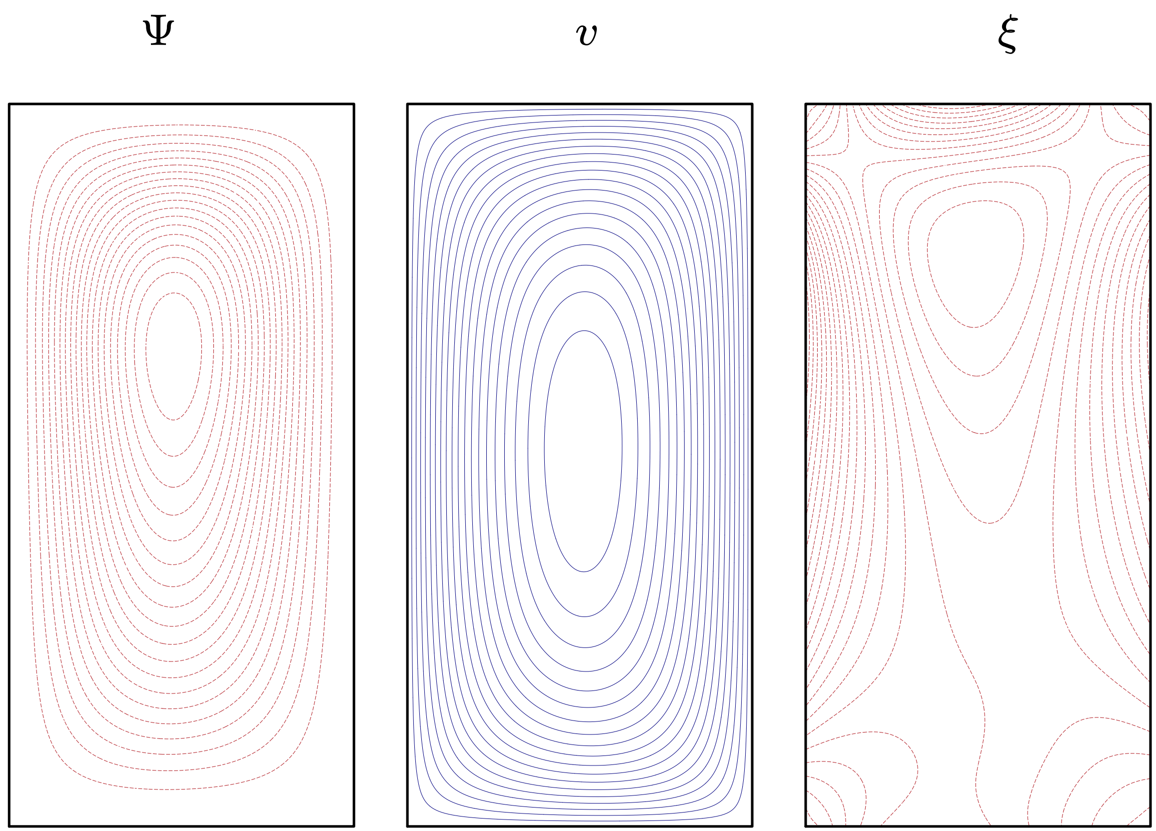

Flow and hydrodynamic instability

Flow structure in the tall pipe $(\phi_0 = \pi)$

$\mathbf{R_e = 22}$

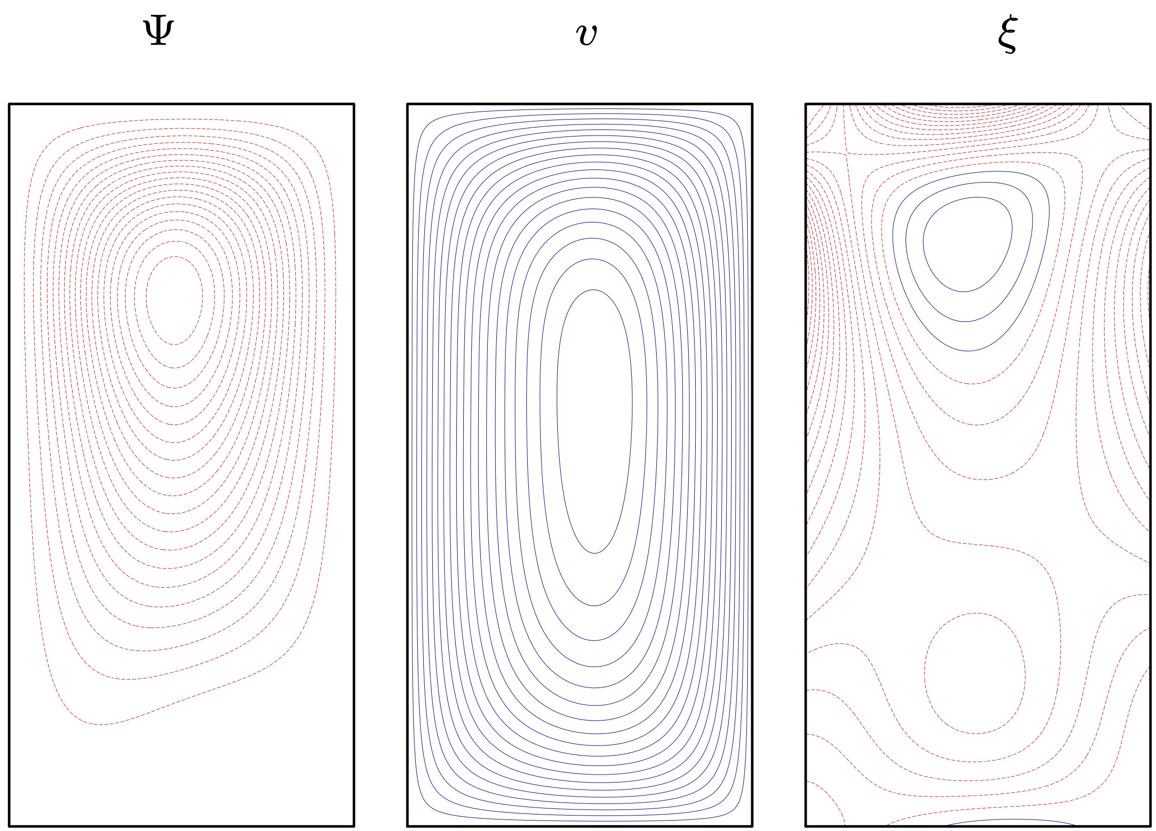

Sizable second ψ-gyre has just appeared. Dynamo now possible.

Flow and hydrodynamic instability

Flow structure in the tall pipe $(\phi_0 = \pi)$

$\mathbf{R_e = 27}$

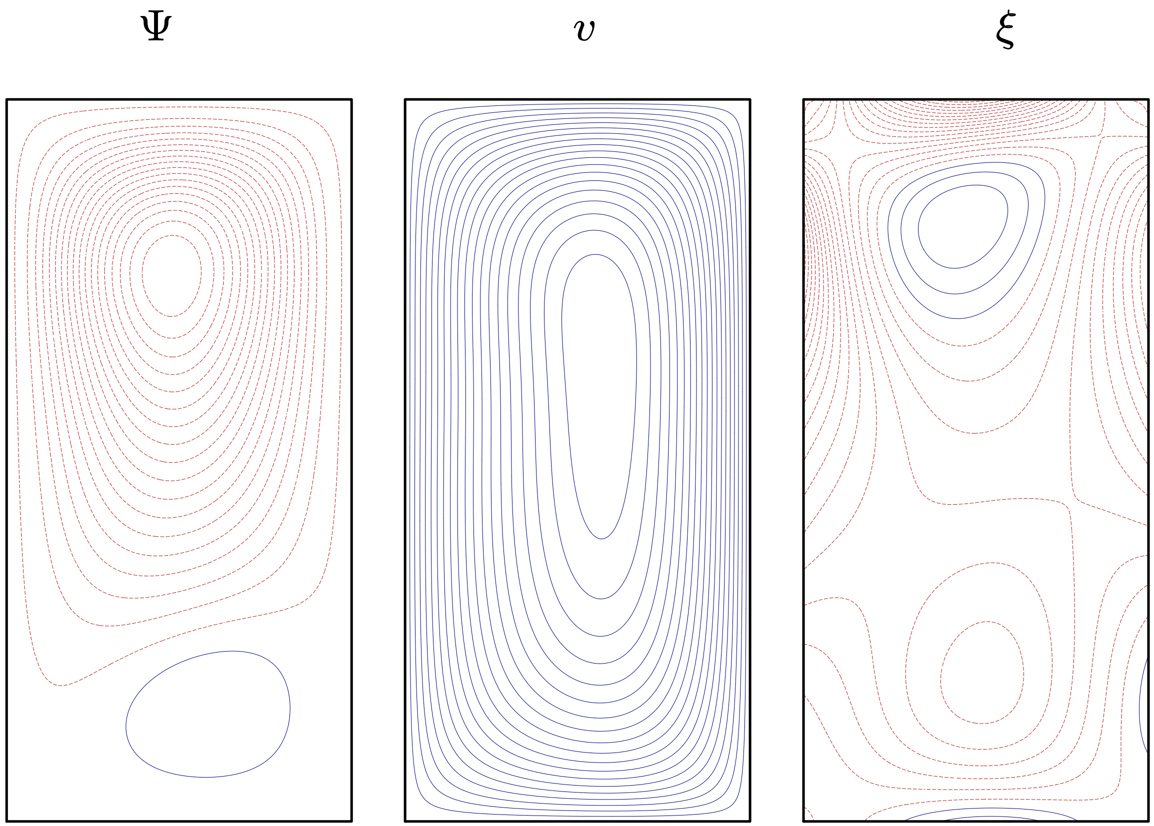

Flow and hydrodynamic instability

Flow structure in the tall pipe $(\phi_0 = \pi)$

$\mathbf{R_e = 38}$

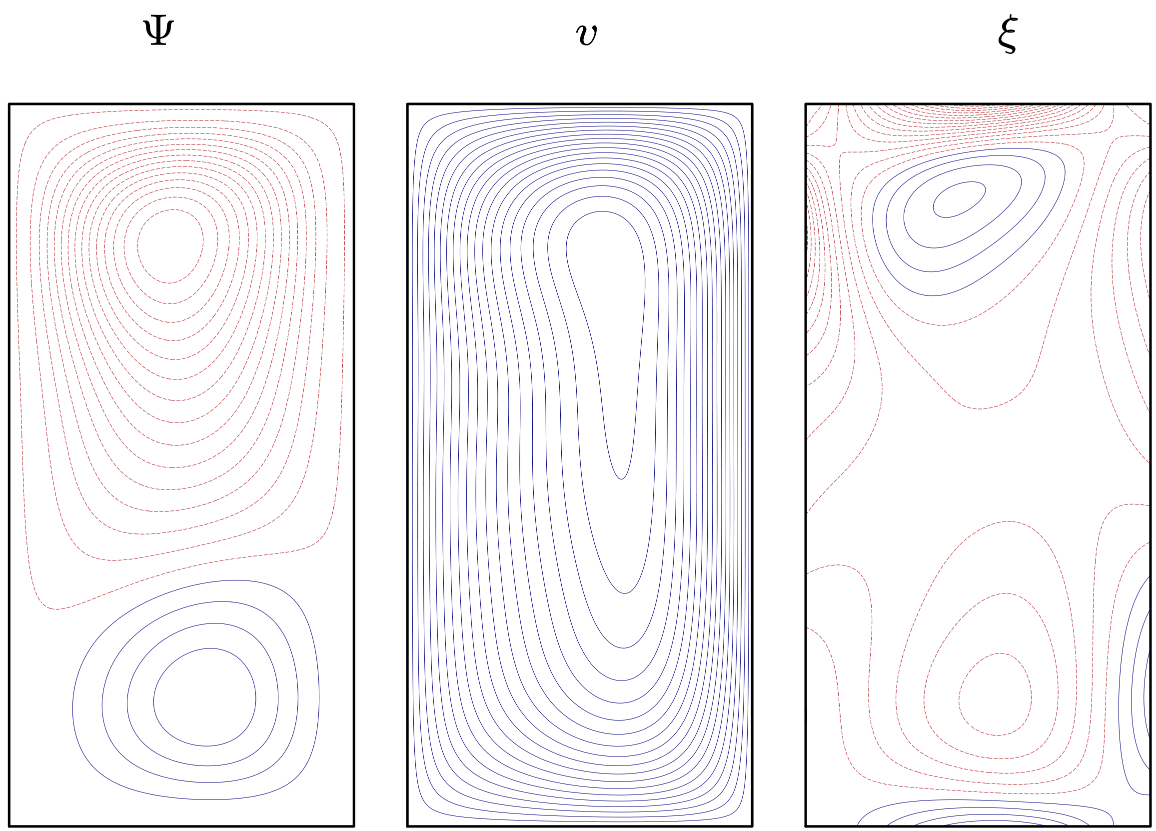

Flow and hydrodynamic instability

Flow structure in the tall pipe $(\phi_0 = \pi)$

$\mathbf{R_e = 49}$

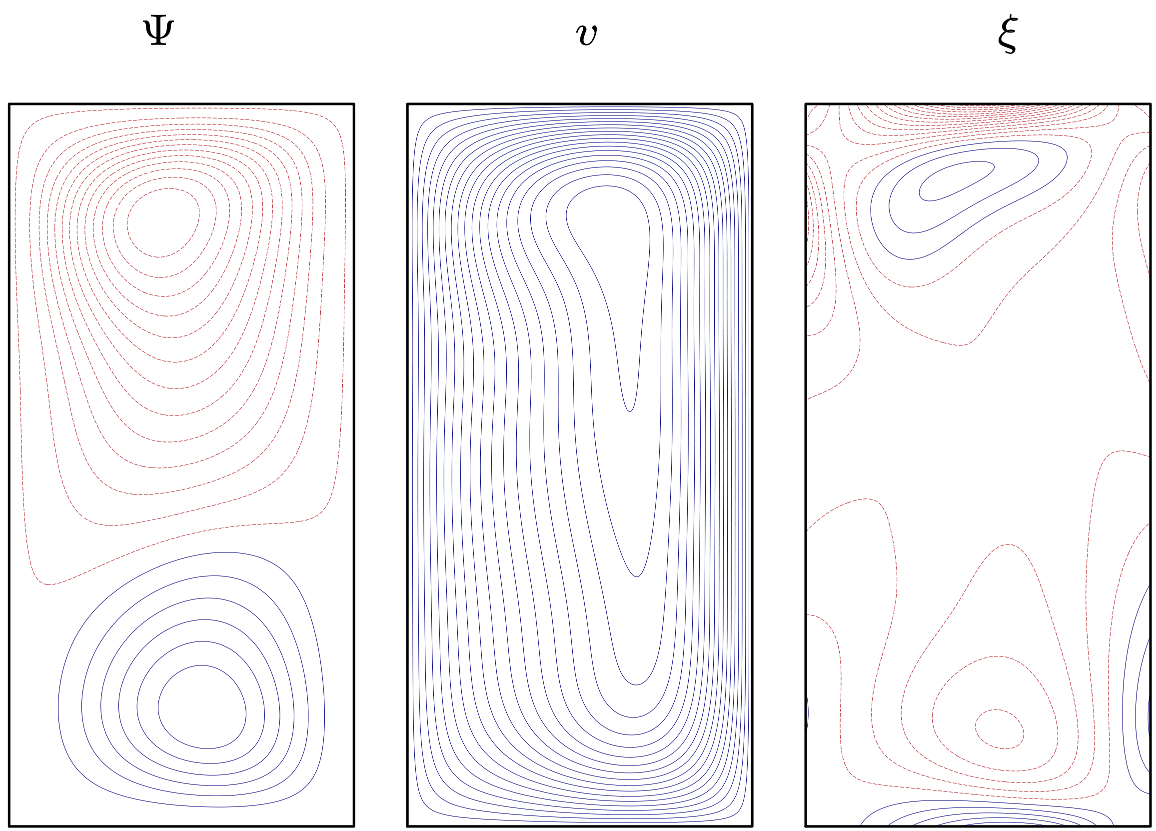

Flow and hydrodynamic instability

Flow structure in the tall pipe $(\phi_0 = \pi)$

$\mathbf{R_e = 69}$

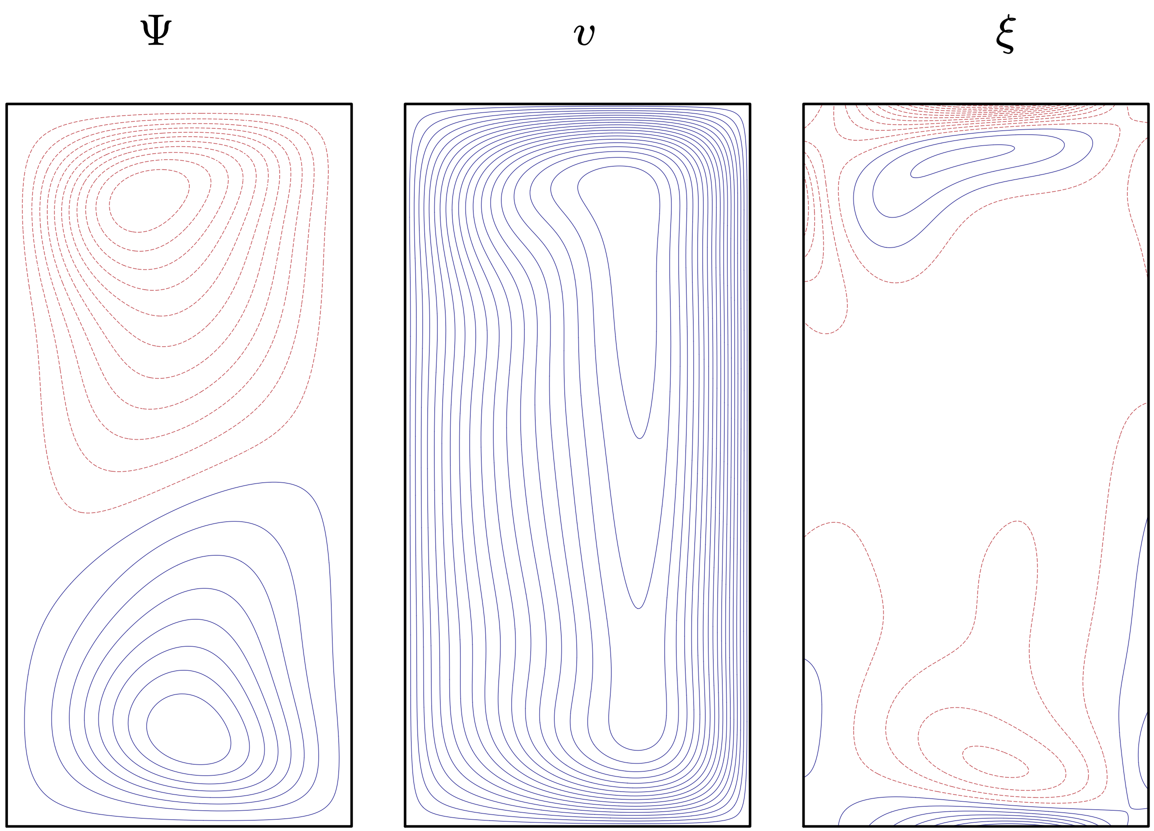

As R_e increases the flow becomes unsteady. A hydrodynamic instability develops
c.f. Hall and Horseman (1991), $\mathbf{R_e = 83}$ $\mathbf{R_e = 106}$

Nonlinear helical dynamo in a single pipe

Perfectly conducting walls. $\mathbf{R_e = 37}\ \phi_0 = \frac{\mathbf{2}\pi}{\mathbf{3}}$

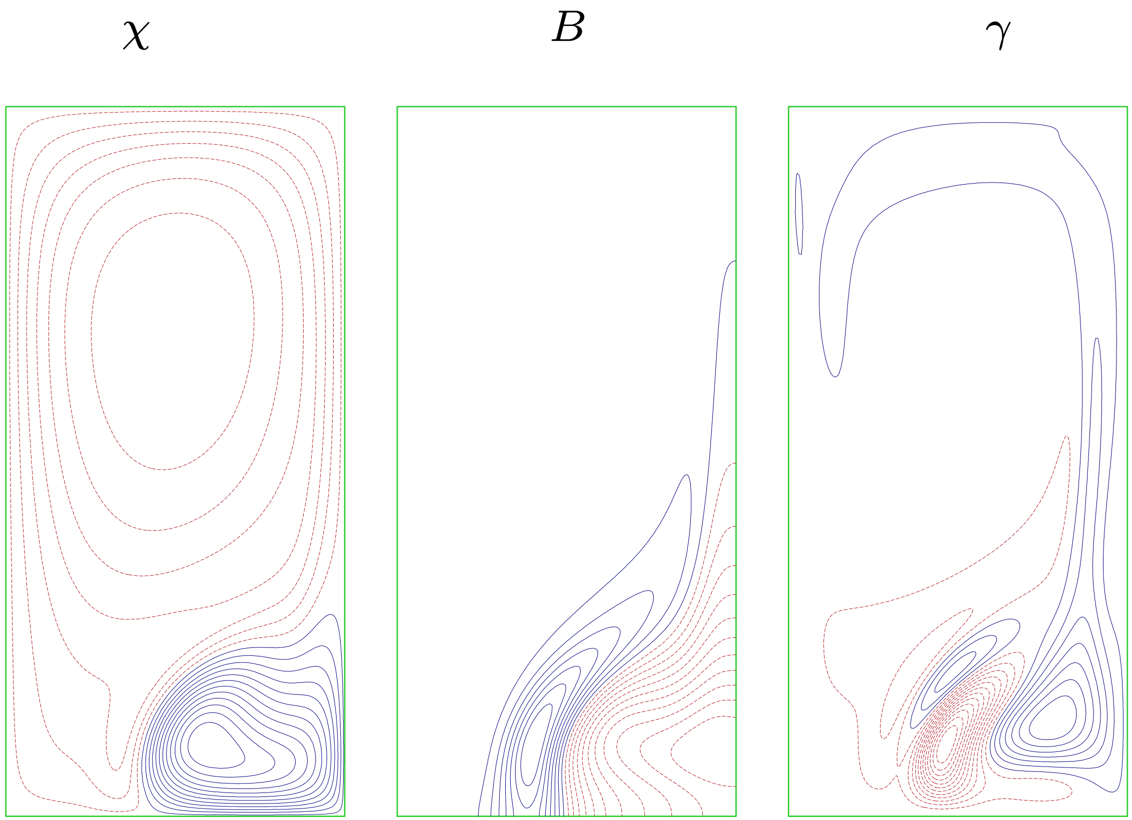

Unique laminar flow: Kinematic dynamo always extends to fully nonlinear regime.

Eigenfunction evolution

Energy traces for single-pipe dynamo

$$E_k = \frac{1}{2}\int_V |\mathbf{u}|^2 \, dV \quad \text{(red)} \qquad E_m = \frac{1}{2}\int_V |\mathbf{B}|^2 \, dV \quad \text{(blue)}$$

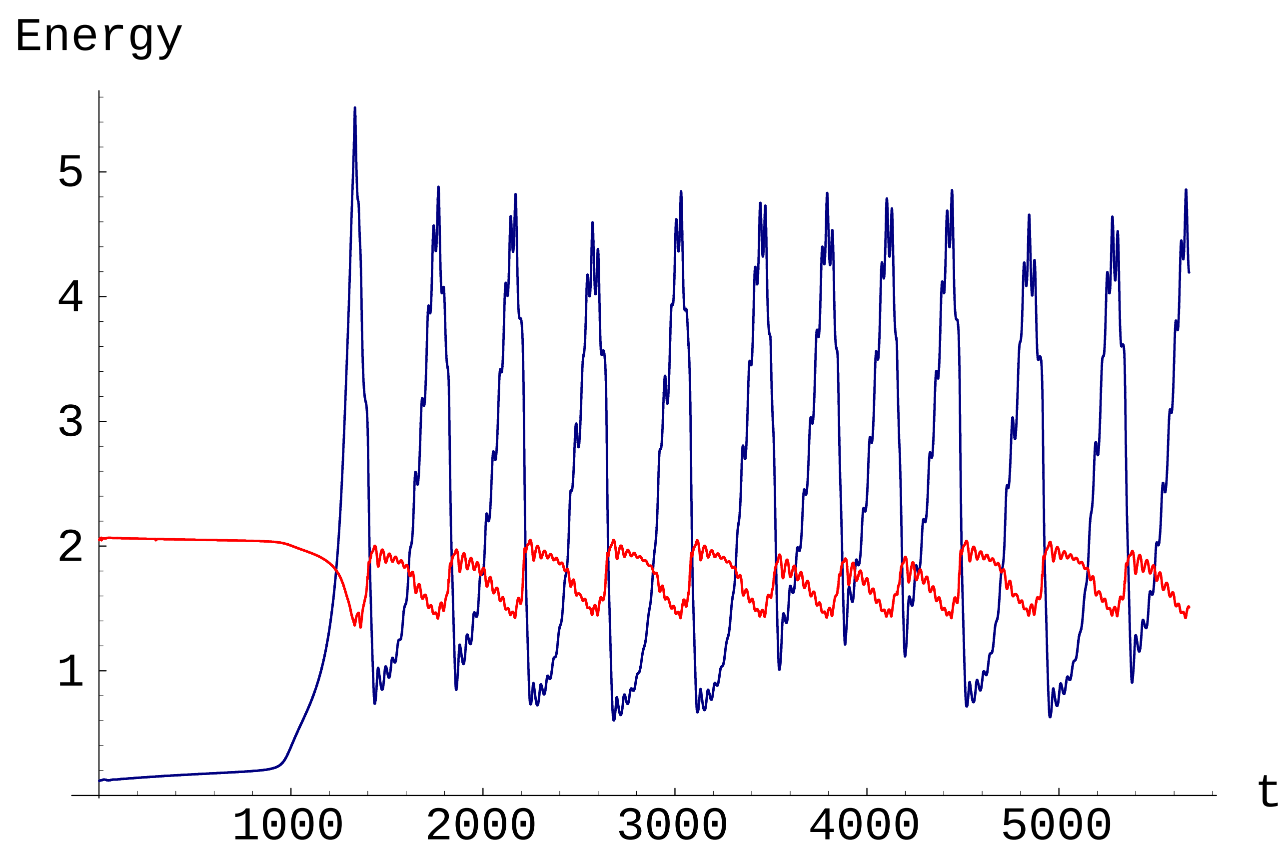

$\mathbf{R_m = 11.4^3}$

Time evolution (field reversal)

Energy traces for single-pipe dynamo

$$E_k = \frac{1}{2}\int_V |\mathbf{u}|^2\, dV \quad \text{(red)} \qquad E_m = \frac{1}{2}\int_V |\mathbf{B}|^2\, dV \quad \text{(blue)}$$

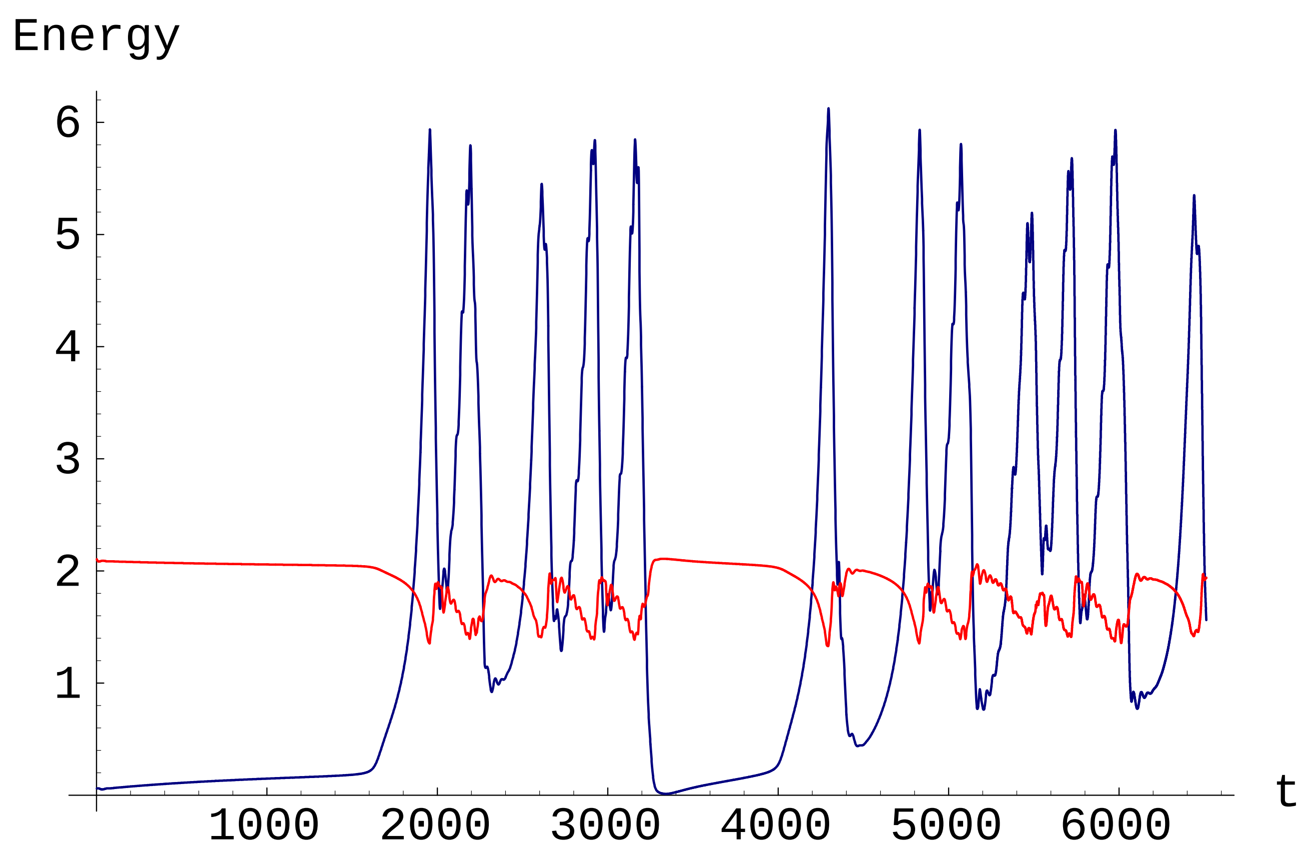

$\mathbf{R_m = 12^3}$

Energy traces for single-pipe dynamo

$E_k = \frac{1}{2}\int_V |\mathbf{u}|^2 \, dV$ (red) $\qquad E_m = \frac{1}{2}\int_V |\mathbf{B}|^2 \, dV$ (blue)

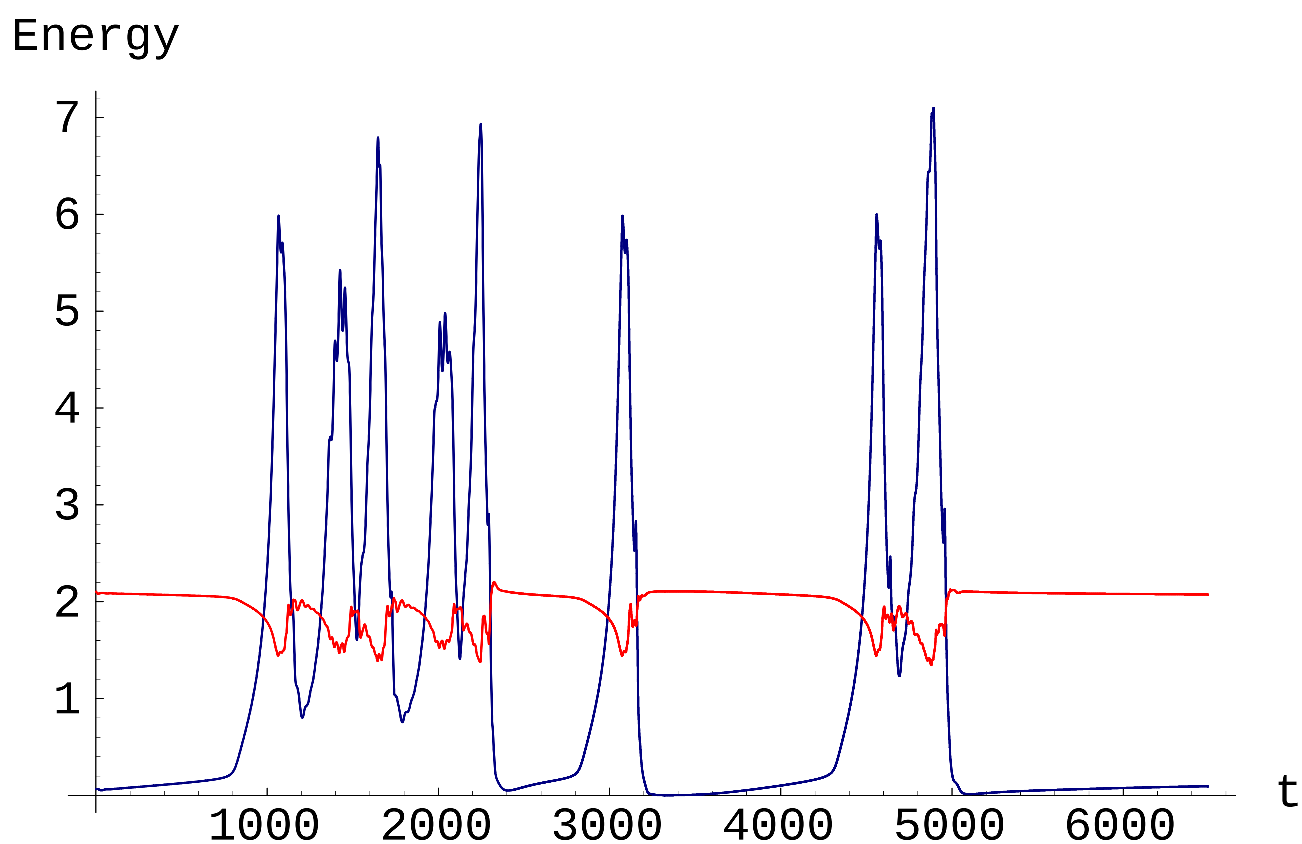

$\mathbf{R_m = 13^3}$

Time evolution magnetic quenching

Single-pipe energy balance

$$\frac{dE_k}{dt} = Q(t) + \int_V \mathbf{u}\cdot\mathbf{j}\times\mathbf{B}\,\mathrm{d}V - \nu\int_V |\boldsymbol{\omega}|^2\,\mathrm{d}V$$

where Q denotes the volume flux down the pipe

$$\frac{dE_m}{dt} = -\int_V \mathbf{u}\cdot\mathbf{j}\times\mathbf{B}\,\mathrm{d}V - \eta\int_V |\mathbf{j}|^2\,\mathrm{d}V$$

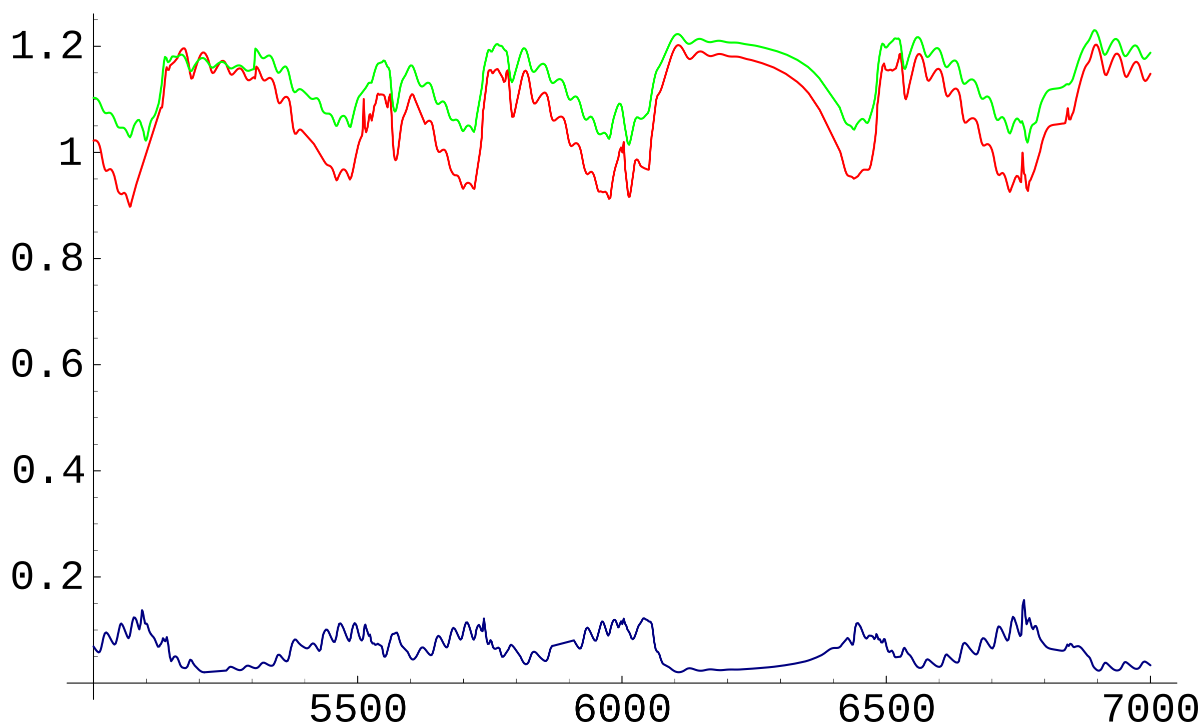

$R_m = 12^3$

The double-helix dynamo

Two helical pipes are interwoven as in the figure so as to completely fill the cylindrical annulus $R_1 < r < R_2$. The flow is driven in opposite directions in each pipe. The cylinder walls ($r =$ const) are perfectly conducting. The magnetic field could have the same up-down symmetry or the opposite.

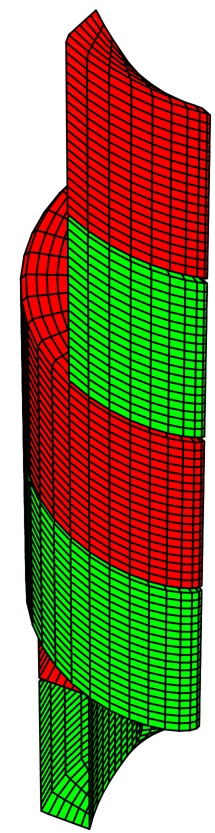

$$\frac{\partial B}{\partial \phi} = 0, \quad \frac{\partial \chi}{\partial \phi} = 0, \quad \text{on } \phi = 0, \pi \qquad \text{symmetric}$$

$$B = 0, \quad \chi = 0 \quad \text{on } \phi = 0, \pi \qquad \text{antisymmetric}$$

The symmetric eigenfunctions
are found to have a significantly larger growth rate.
Calculations over the double-helix also prefer this symmetry.

The double-helix dynamo

Two helical pipes are interwoven as in the figure so as to completely fill the cylindrical annulus $R_1 < r < R_2$. The flow is driven in opposite directions in each pipe. The cylinder walls ($r =$ const) are perfectly conducting. The magnetic field could have the same up-down symmetry or the opposite.

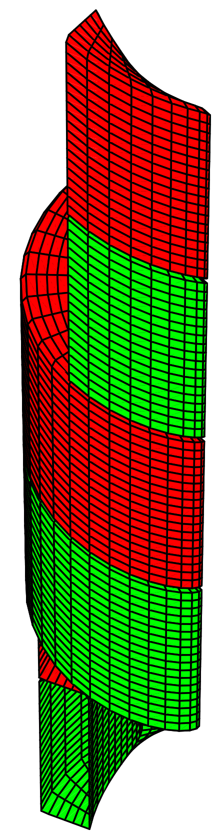

$$\frac{\partial B}{\partial \phi} = 0, \quad \frac{\partial \chi}{\partial \phi} = 0, \quad \text{on } \phi = 0, \pi \qquad \text{symmetric}$$

$$B = 0, \quad \chi = 0 \quad \text{on } \phi = 0, \pi \qquad \text{antisymmetric}$$

The symmetric eigenfunctions
are found to have a significantly larger growth rate.
Calculations over the double-helix also prefer this symmetry.

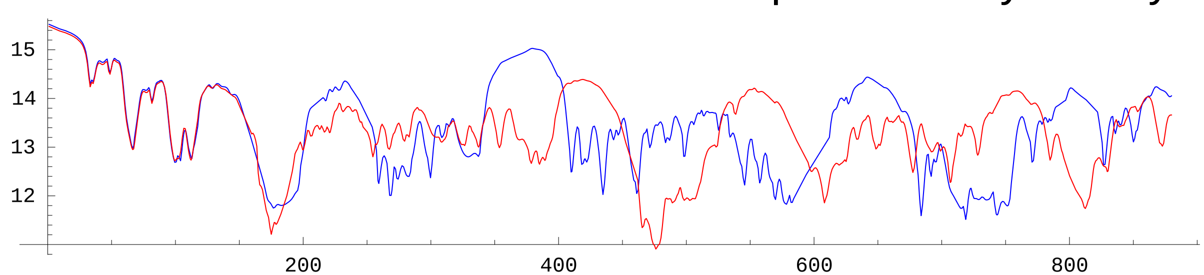

Dynamo region for double helix

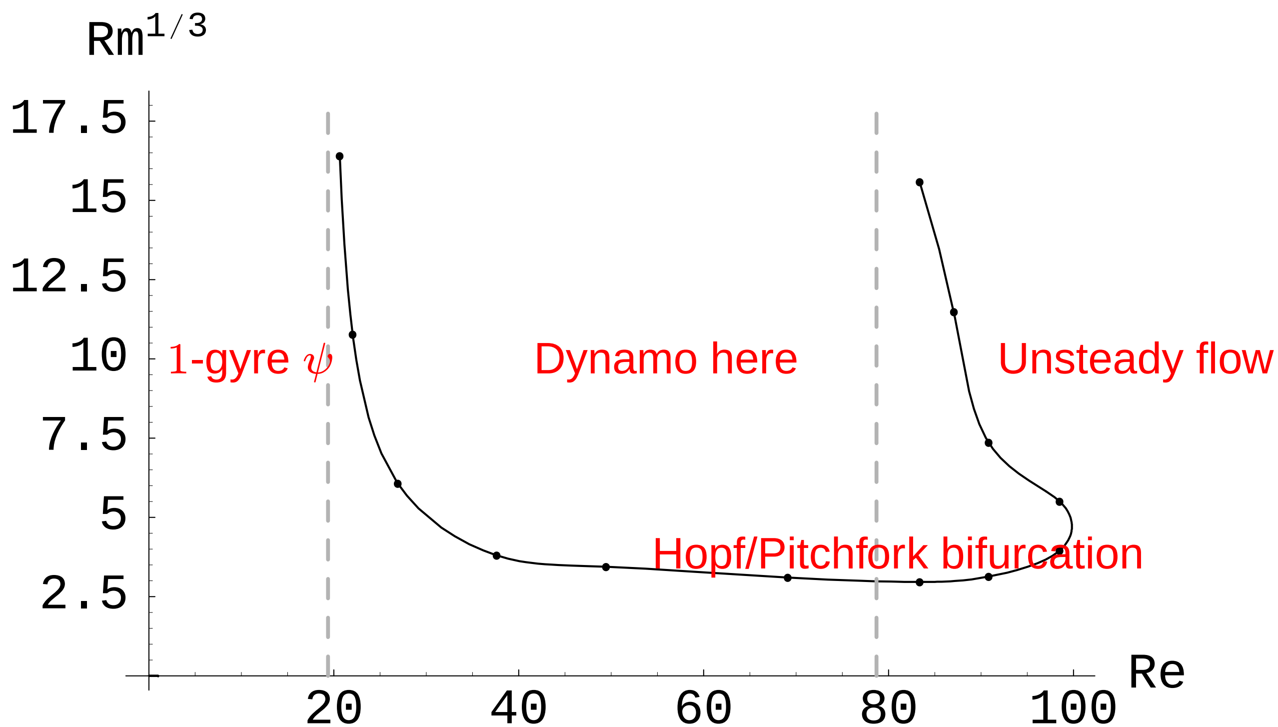

In the double helix, dynamo action occurs for a wider range of Reynolds numbers than for the single-pipe dynamo. The dynamo fails when the flow becomes unsteady due to a centrifugal hydrodynamic instability that develops on the outer wall.

Dynamical Systems aspects of two-pipe problem

- **Hopf/Pitchfork bifurcation** occurs at $R_e \simeq 80$, $R_m \simeq 27$. The minimum critical R_m occurs above the critical R_e.
- **Hopf/Hopf** bifurcation occurs for different magnetic boundary conditions.
- **Symmetry:** Magnetic field prefers the same symmetry as the velocity field.
- **Phase locking**: The steady flows in the two pipes are the same, but there is no reason why the unsteady flows should be in phase. Nonlinear dynamo effects can lead to phase-locking between the two pipe flows, and indeed to
- **Flow stabilisation**. Steady saturated dynamo states are possible for supercritical R_e. Likewise, a-periodic flows can be rendered periodic.
- **Dynamo pump**: Flow driven down just one pipe can still give rise to a dynamo. The induced Lorentz force can then drive flow in the second pipe. In the case we investigated, the driven mean flow was in the same direction. (c.f. MREP's secret)
- **Field reversals & quenching** Unlike the single pipe dynamo, field reversals do not seem to occur. Intermittent quenching can still occur.

Double helix dynamo

Energy traces

$$E_k = \frac{1}{2}\int_V |\mathbf{u}|^2 \, dV \quad \text{(red)} \qquad E_m = \frac{1}{2}\int_V |\mathbf{B}|^2 \, dV \quad \text{(blue)}$$

R_e =69

$$\mathbf{R_m = 3.7^3}$$

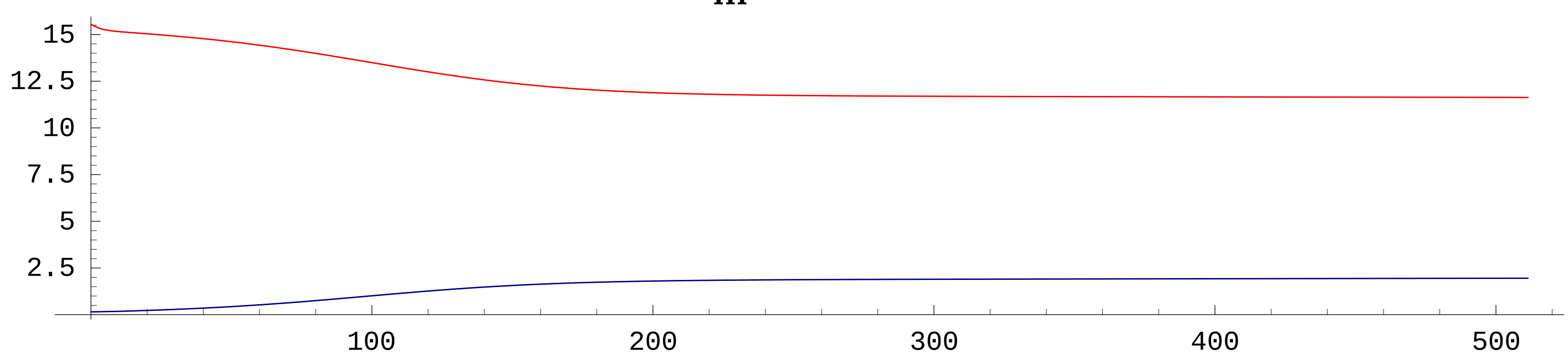

Steady state

Double helix dynamo

Energy traces

$$E_k = \frac{1}{2}\int_V |\mathbf{u}|^2 \, dV \quad \text{(red)} \qquad E_m = \frac{1}{2}\int_V |\mathbf{B}|^2 \, dV \quad \text{(blue)}$$

R_e =69

$\mathbf{R_m = 5^3}$

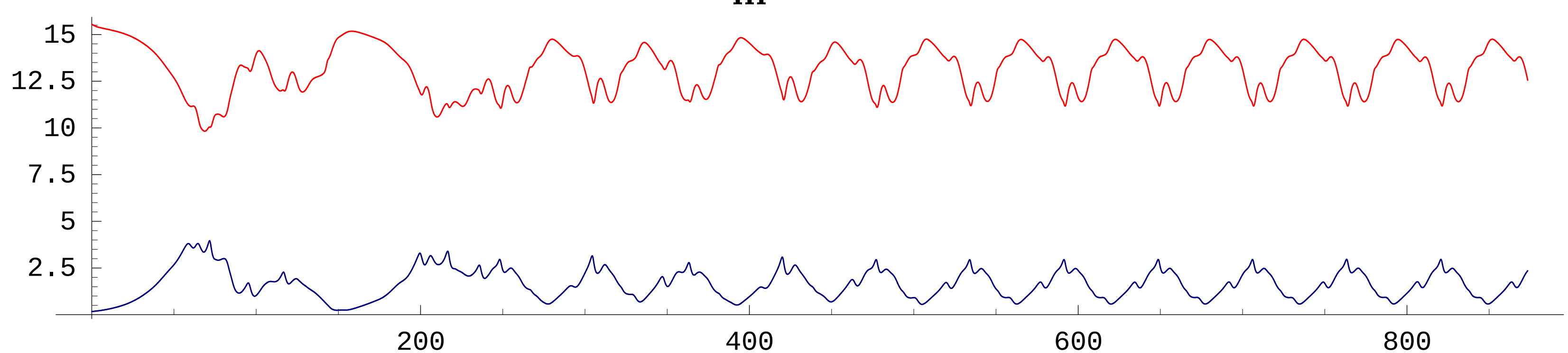

periodic behaviour

Double helix dynamo

Energy traces

$$E_k = \frac{1}{2}\int_V |\mathbf{u}|^2\, dV \quad \text{(red)} \qquad E_m = \frac{1}{2}\int_V |\mathbf{B}|^2\, dV \quad \text{(blue)}$$

R_e =69

$\mathbf{R_m = 7^3}$

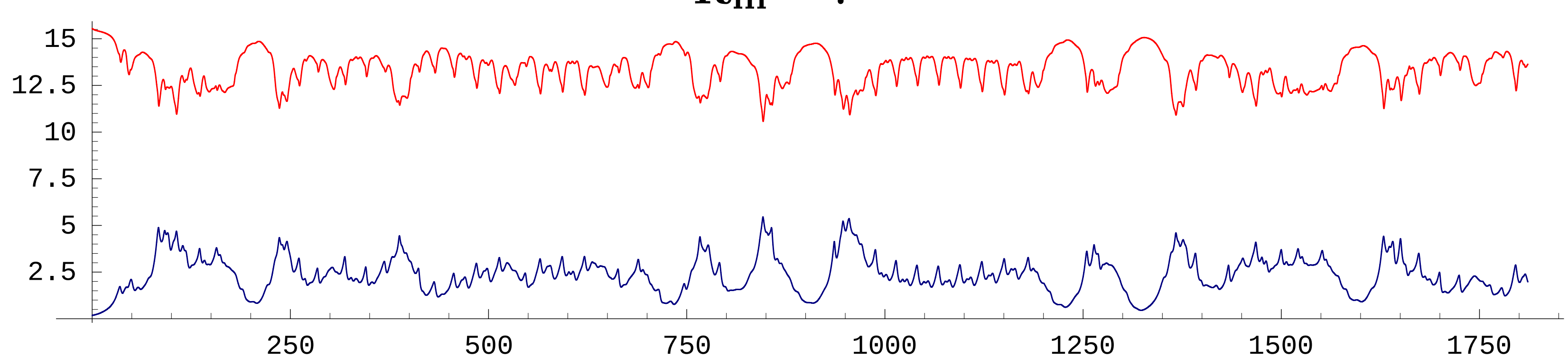

Quasiperiodic solution

Double helix dynamo

Energy traces

$$E_k = \frac{1}{2}\int_V |\mathbf{u}|^2\, dV \quad \text{(red)} \qquad E_m = \frac{1}{2}\int_V |\mathbf{B}|^2\, dV \quad \text{(blue)}$$

R_e =69

$\mathbf{R_m = 10^3}$

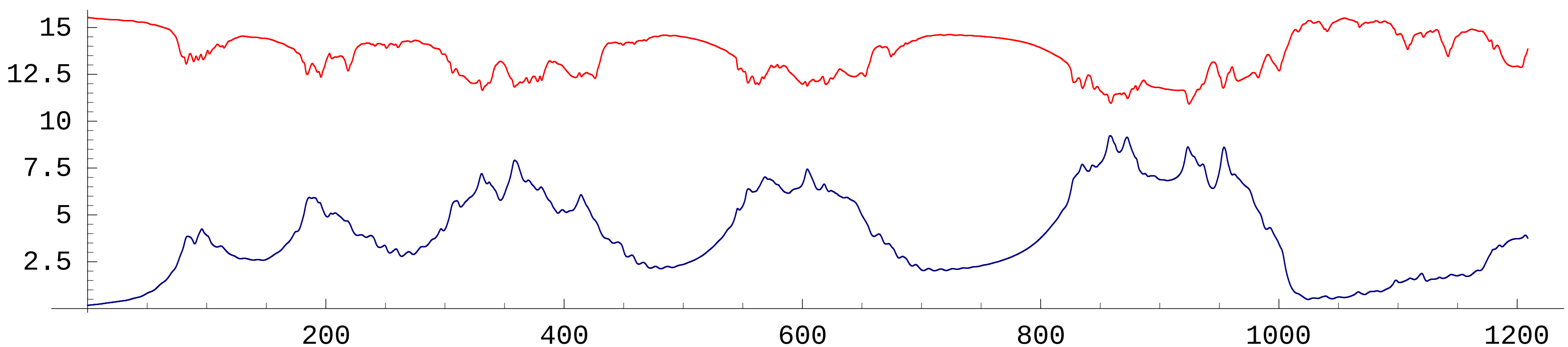

Double helix dynamo

Energy traces

$$E_k = \frac{1}{2}\int_V |\mathbf{u}|^2\, dV \quad \text{(red)} \qquad E_m = \frac{1}{2}\int_V |\mathbf{B}|^2\, dV \quad \text{(blue)}$$

R_e =69

$\mathbf{R_m = 14^3}$

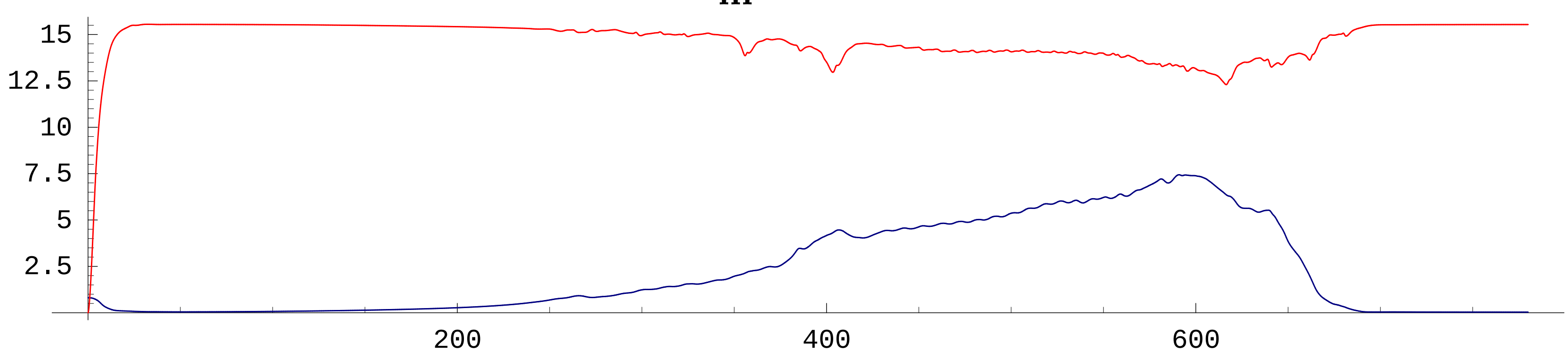

Quenching

Double helix dynamo

Energy traces

$$E_k = \frac{1}{2}\int_V |\mathbf{u}|^2\, dV \quad \text{(red)} \qquad E_m = \frac{1}{2}\int_V |\mathbf{B}|^2\, dV \quad \text{(blue)}$$

R_e =69

$\mathbf{R_m = 15^3}$

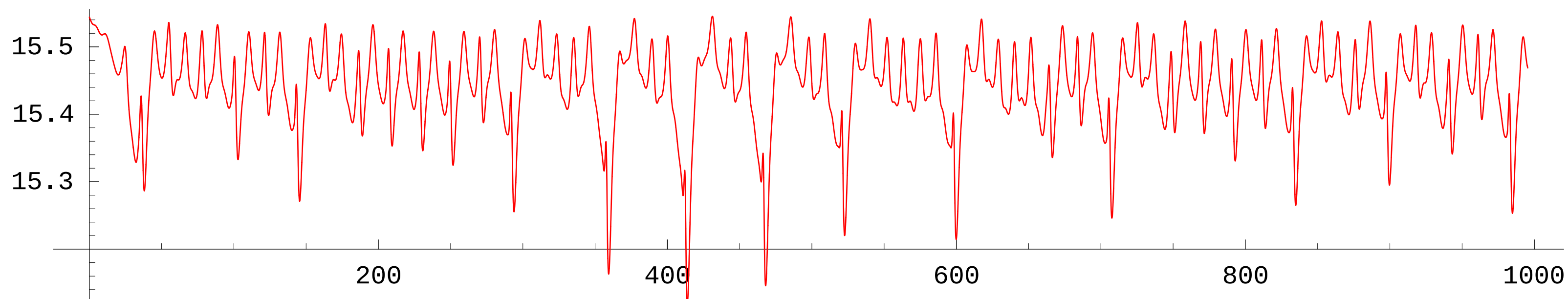

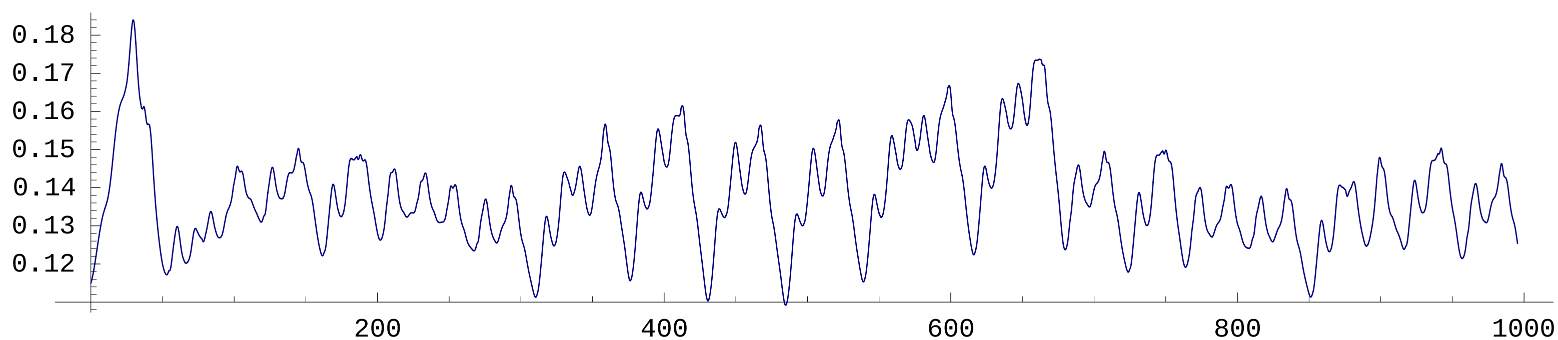

Double helix dynamo

Energy traces

$$E_k = \frac{1}{2}\int_V |\mathbf{u}|^2\, dV \quad \text{(red)} \qquad E_m = \frac{1}{2}\int_V |\mathbf{B}|^2\, dV \quad \text{(blue)}$$

R_e =69

$\mathbf{R_m = 20^3}$

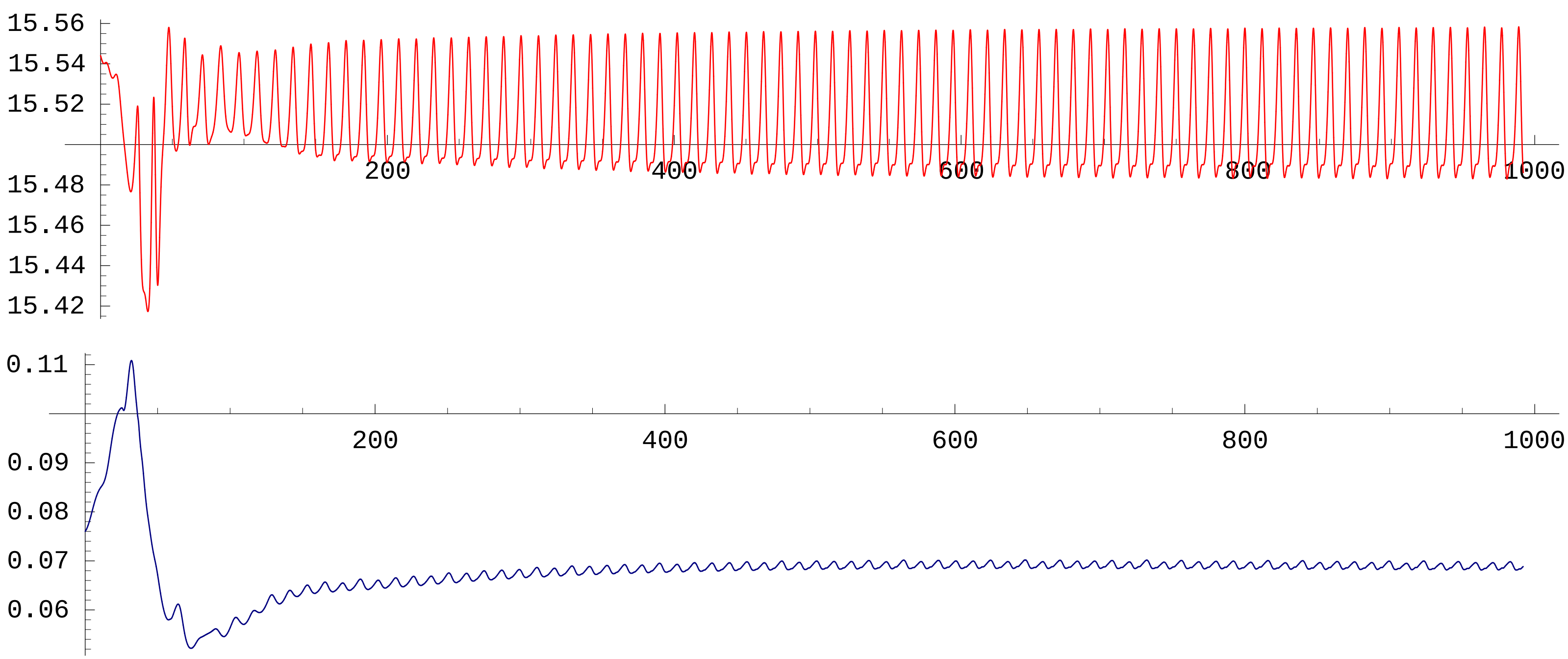

As R_m increases dynamo becomes periodic with low E_m

Double helix dynamo

Energy traces

$$E_k = \frac{1}{2}\int_V |\mathbf{u}|^2 \, dV \quad \text{(red)} \qquad E_m = \frac{1}{2}\int_V |\mathbf{B}|^2 \, dV \quad \text{(blue)}$$

R_e =27

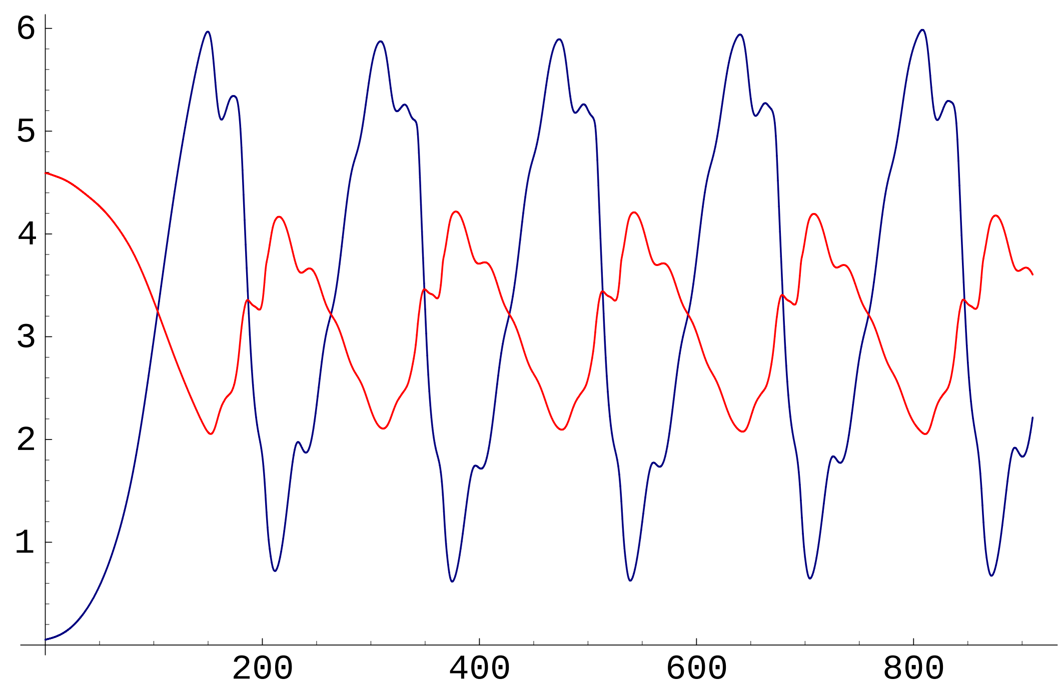

Time evolution (periodic behaviour)

Double helix dynamo

Energy traces

$$E_k = \frac{1}{2}\int_V |\mathbf{u}|^2\, dV \quad \text{(red)} \qquad E_m = \frac{1}{2}\int_V |\mathbf{B}|^2\, dV \quad \text{(blue)}$$

R_e =27

$$\mathbf{R_m = 20^3}$$

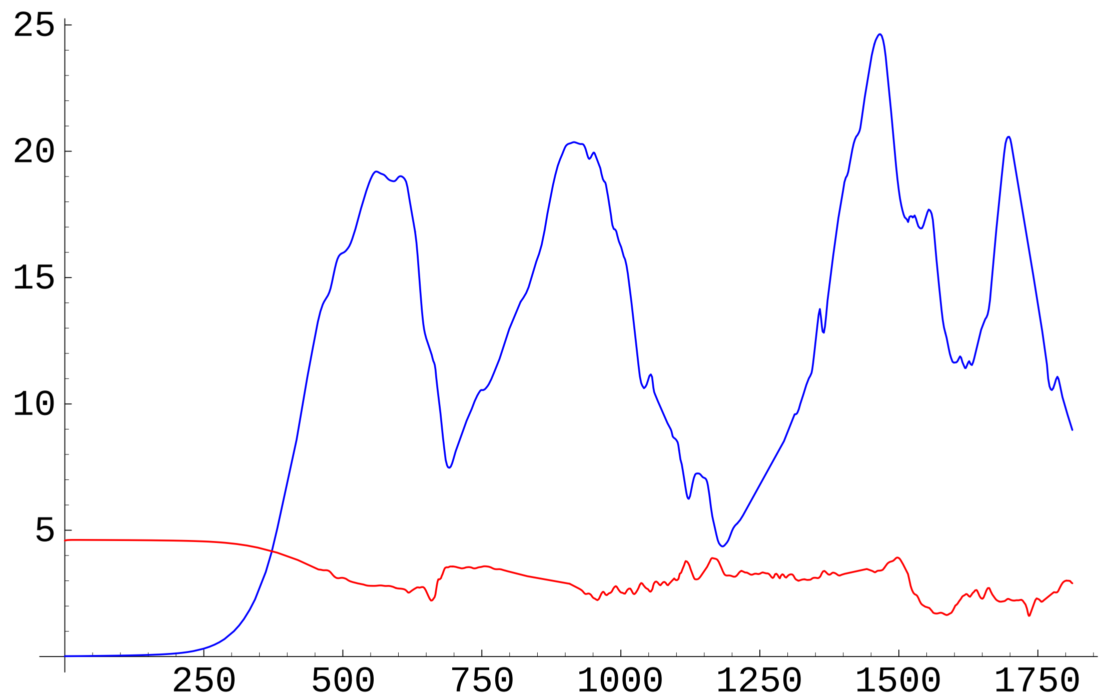

Time evolution 1 2

How to reach low magnetic Prandtl number?

The double-helix dynamo works for $R_m > 30$ and a magnetic Prandtl number $R_m/R_e > 0.5$. For liquid metals R_m/R_e should be much lower.

How can we achieve a laminar, low-Prandtl number dynamo?

How to reach low magnetic Prandtl number?

The double-helix dynamo works for $R_m > 30$ and a magnetic Prandtl number $R_m/R_e > 0.5$. For liquid metals R_m/R_e should be much lower.

How can we achieve a laminar, low-Prandtl number dynamo?

"That sounds like more than a two-pipe problem, Watson. . . "

Conan-Doyle (1891).

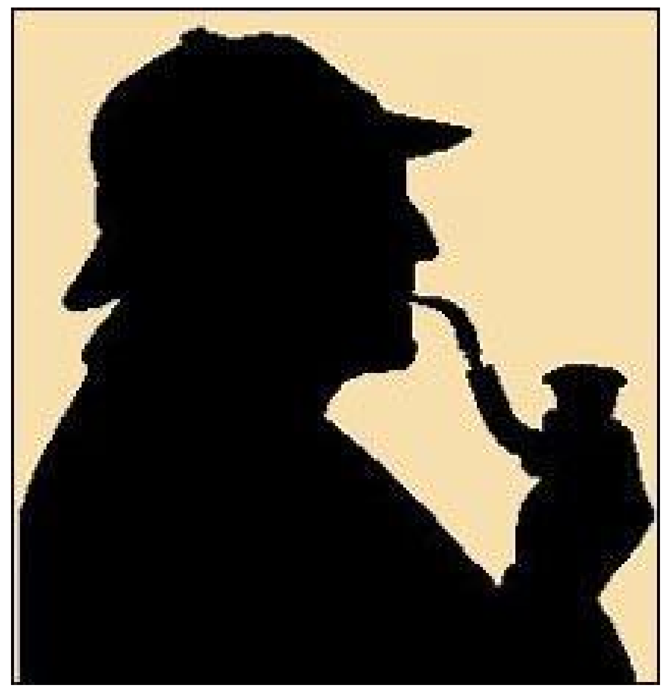

[compare MREP J. Caesar, 50 B.C.]

Multi-pipe dynamos

The tall pipes in the double-helix dynamo are prone to Görtler instabilities on the curved outer wall. This instability is unfavourable for dynamo action.

Dynamos in multiple, shorter pipes appear more robust. The unsteady flows which arise have a travelling wave character which still drives a dynamo.

This example was created recently for a 16-pipe configuration:

16-pipe dynamo

Asymptotically, we can analyse the stability of these almost parallel short pipe flows:

Orr-Sommerfeld equations for large number of pipes

We can solve these coupled equations using standard Orr-Sommerfeld spectral techniques - 100 Chebyshev modes in the ϕ-direction reduce the problem to the generalised matrix eigenvalue problem

$$\begin{pmatrix} A_1 & A_2 \\ A_3 & A_4 \end{pmatrix} \begin{pmatrix} \psi \\ v \end{pmatrix} = s \begin{pmatrix} B & 0 \\ 0 & I \end{pmatrix} \begin{pmatrix} \psi \\ v \end{pmatrix}$$

We find the neutral stability curve, whose shape resembles strongly that for the inflectional cross-pipe flow.

The eigenvalue spectra for different numbers of modes provides an accuracy check, plotted in the complex s-plane for $R_e = 75$, $k = 2$, which is just stable.

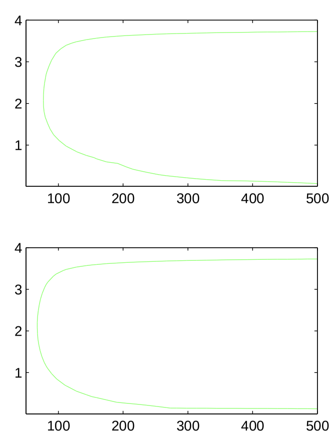

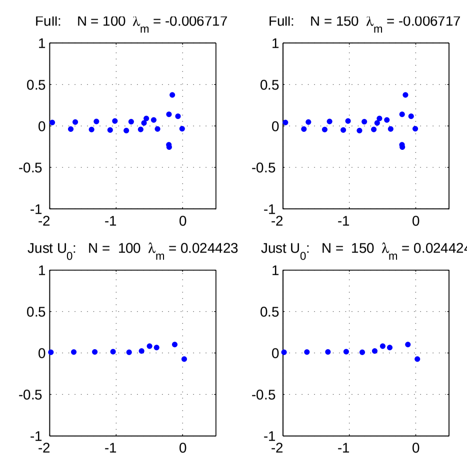

Orr-Sommerfeld equations for large number of pipes

Neutral stability curve, $\Re e(s) = 0$

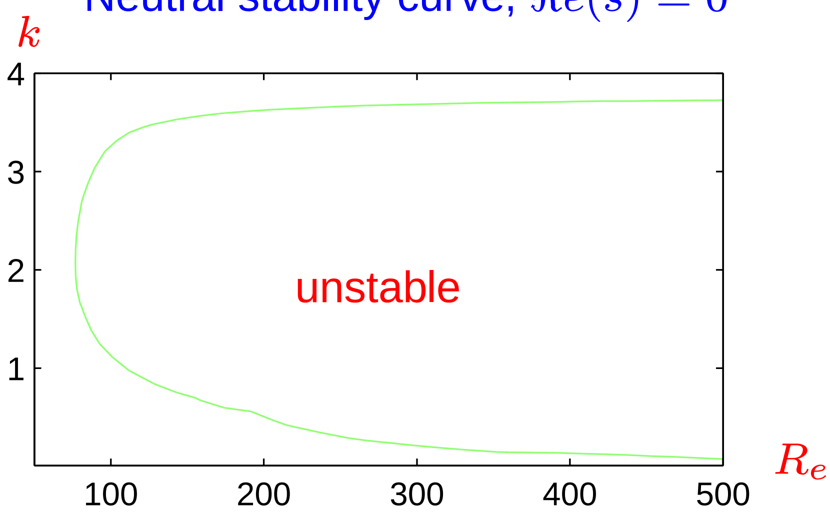

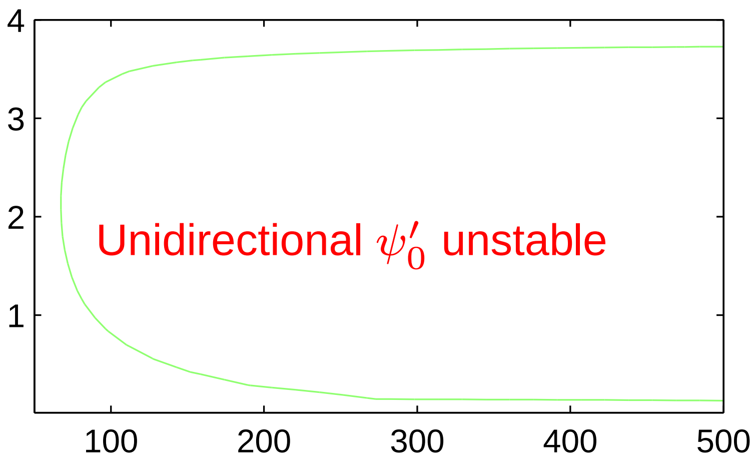

Conclusions

These helical pipe dynamos have one big advantage and one big disadvantage:

Conclusions

These helical pipe dynamos have one big advantage and one big disadvantage:

ADVANTAGE: They are laminar

Thus they are exact solutions of the Navier Stokes and induction equations which can be extended into the nonlinear regime.

I believe they are the only known laminar, pressure driven dynamos.

However, non-uniqueness implies that they may not occur in practice. Indeed, the preferred magnetic field configuration may not even be helically symmetric. But the existence of these solutions implies that a sustainable dynamo of some sort exists, for $R_m \simeq 30$. The solutions exhibit Field reversals, magnetic quenching, periodic and quasiperiodic behaviour.

Conclusions

These helical pipe dynamos have one big advantage and one big disadvantage:
ADVANTAGE: They are laminar
Thus they are exact solutions of the Navier Stokes and induction equations which can be extended into the nonlinear regime.
I believe they are the only known laminar, pressure driven dynamos.
However, non-uniqueness implies that they may not occur in practice. Indeed, the preferred magnetic field configuration may not even be helically symmetric. But the existence of these solutions implies that a sustainable dynamo of some sort exists, for $R_m \simeq 30$. The solutions exhibit Field reversals, magnetic quenching, periodic and quasiperiodic behaviour.

DISADVANTAGE: They are laminar
In reality, the magnetic Prandtl number is such that we know the real liquid metal flow would be turbulent. The multiple pipe dynamos function at $Pr_m < 0.01$ and survives some but not all flow instabilities. As R_e increases still further the dynamo is still destroyed.